JOINT TRANSPORTATION
RESEARCH PROGRAM
INDIANA DEPARTMENT OF TRANSPORTATION
AND PURDUE UNIVERSITY

Influence of Nanomaterials-Based Admixtures and Polymeric Microspheres on Entrained Air Void System and Freeze-Thaw (F/T) Resistance of Concrete

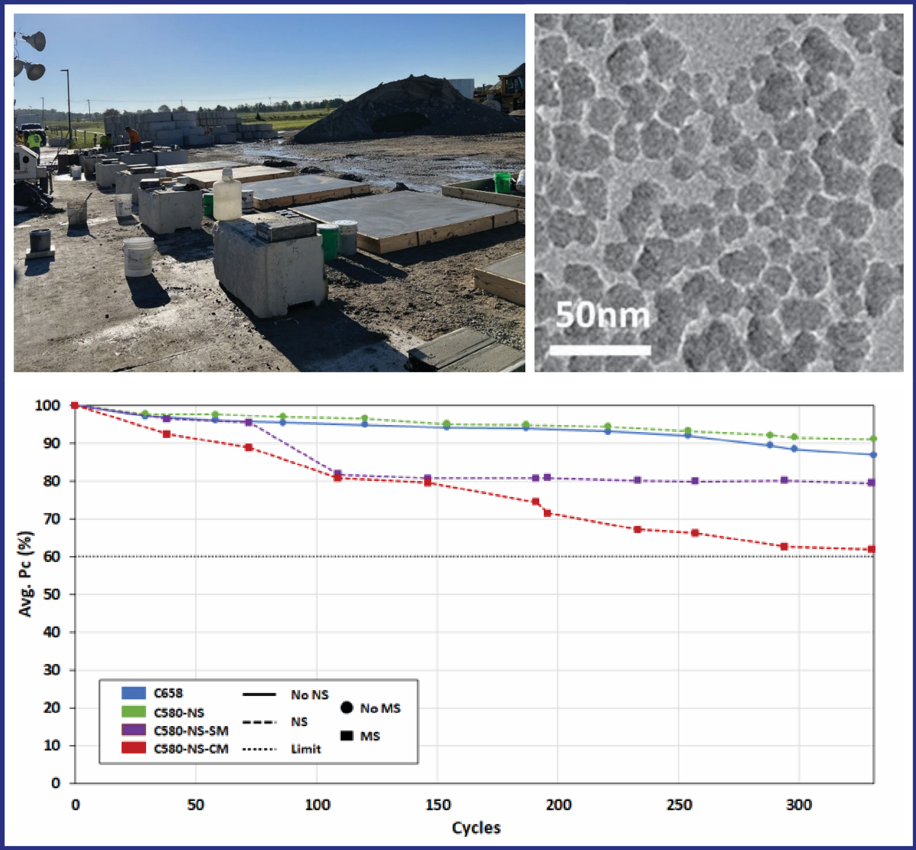

Alberto Castillo, Jan Olek, and Mirian Velay-Lizancos

SPR-4718 • Report Number: FHWA/IN/JTRP-2026/13 • DOI: 10.5703/1288284318621

RECOMMENDED CITATION

Castillo, A., Olek, J., & Velay-Lizancos, M. (2026). *Influence of nanomaterials-based admixtures and polymeric microspheres on entrained air void system and freeze-thaw (F/T) resistance of concrete* (Joint Transportation Research Program Publication No. FHWA/IN/JTRP-2026/13). West Lafayette, IN: Purdue University. https://doi.org/10.5703/1288284318621

AUTHORS

Alberto Castillo
Purdue University

Jan Olek
Purdue University
(765) 494-5015
olek@purdue.edu
Corresponding Author

Mirian Velay-Lizancos
Purdue University

JOINT TRANSPORTATION RESEARCH PROGRAM

The Joint Transportation Research Program serves as a vehicle for INDOT collaboration with higher education institutions and industry in Indiana to facilitate innovation that results in continuous improvement in the planning, design, construction, operation, management and economic efficiency of the Indiana transportation infrastructure. Learn more at engineering.purdue.edu/JTRP.

Published reports of the Joint Transportation Research Program are available at docs.lib.purdue.edu/jtrp/.

NOTICE

TECHNICAL REPORT DOCUMENTATION PAGE

1. Report No.	2. Government Accession No.	3. Recipient's Catalog No.
FHWA/IN/JTRP-2026/13		

4. Title and Subtitle
Influence of nanomaterials-based admixtures and polymeric microspheres on entrained air void system and freeze-thaw (F/T) resistance of concrete

5. Report Date
February 26, 2026

6. Performing Organization Code

7. Author(s)
Alberto Castillo, PhD (https://orcid.org/0009-0000-0959-8684)
Jan Olek, PhD (https://orcid.org/0000-0003-0467-9877)
Mirian Velay-Lizancos, PhD (https://orcid.org/0000-0002-1539-7923)

8. Performing Organization Report No.
FHWA/IN/JTRP-2026/13

9. Performing Organization Name and Address
Joint Transportation Research Program
Hall for Discovery and Learning Research (DLR), Suite 204
207 S. Martin Jischke Drive
West Lafayette, IN 47907

10. Work Unit No.

11. Contract or Grant No.
SPR-4718

12. Sponsoring Agency Name and Address
Indiana Department of Transportation (SPR)
State Office Building
100 North Senate Avenue
Indianapolis, IN 46204

13. Type of Report and Period Covered
Final Report

14. Sponsoring Agency Code

15. Supplementary Notes
Conducted in cooperation with the U.S. Department of Transportation, Federal Highway Administration.

16. Abstract
This study investigated the feasibility of using colloidal nanosilica (nS) as microstructure modifier and polymeric microspheres (MS) as alternative air-entrainment systems for Indiana Department of Transportation (INDOT) bridge deck concrete. These admixtures have gained interest due to their potential to modify the air-void system, enhance freeze-thaw (F/T) resistance, reduce permeability, and improve early-age performance. However, their field applicability depends on understanding their sensitivity to mixture composition, type of batching process, consolidation practices, and water-to-cement (w/c) ratio. The objectives of this research were to: (1) conduct field trials incorporating nS and MS and evaluate both fresh and hardened properties, (2) compare air-void characteristics and F/T performance between field and a companion laboratory mixtures, (3) evaluate the influence of mixing method, compaction effort, and type of batching process on mechanical and durability properties, and (4) quantify the effect of w/c ratio on nS mixtures, including the extent of calcium hydroxide (CH) reduction in paste systems.

Results showed that MS significantly altered the air-void system. Slurry-based MS provided enhanced strength, and reduced secondary rate of water absorption, although F/T performance was highly dependent on MS dispersion and consolidation quality. In laboratory mixtures nanosilica increased water-reducing admixture demand and reduced hardened air content, relative to fresh measurements (no water reducing admixtures were used in field concretes). At the same time, it also produced finer air-void systems (with lower spacing factors), resulting in improved F/T resistance even at reduced total air contents. MS mixtures achieved mechanical properties comparable to or exceeding reference mixtures, while mixes with no nanosilica (nS) showed limited strength benefits. Durability testing indicated reduced secondary absorption and limited chloride ingress (but mostly at greater depths from the surface) for MS mixtures, whereas mixtures containing both ns and MS underperformed with respect to F/T resistance. Paste testing confirmed that using nS resulted only in minor reduction of the CH levels, across all ages and w/c ratios. The observed reductions were substantially lower than those observed in case of using Class C fly ash.

17. Key Words
nanosilica, microspheres, air-entrainment, freeze-thaw resistance, field trials, bridge deck concrete

18. Distribution Statement
No restrictions. This document is available through the National Technical Information Service, Springfield, VA 22161.

19. Security Classif. (of this report)	20. Security Classif. (of this page)	21. No. of Pages	22. Price
Unclassified	Unclassified	33	

Form DOT F 1700.7 (8-72) Reproduction of completed page authorized

EXECUTIVE SUMMARY

Introduction

This study evaluated the performance of concrete mixtures incorporating colloidal nanosilica (nS) and microspheres (MS) as alternative air-entrainment systems for potential use in Indiana Department of Transportation (INDOT) bridge deck concrete. Interest in these admixtures has grown due to their ability to alter the air-void system, improve freeze-thaw (F/T) resistance, reduce permeability, and enhance early-age properties. However, their successful use in practice requires understanding their performance in a field and lab settings, sensitivity to mixture proportioning, and the effect of type of batching process, consolidation, and water-to-cement (w/c) ratio on durability. The main objectives of this study were (1) conduct field trials using nS and MS and retrieve companion cores; (2) compare air-void system and F/T performance of field and lab mixtures; (3) study the effect of mixing method, compaction effort, and batching variability on different mechanical properties and durability; and (4) determine the influence of w/c ratio on mixtures with nS and quantify calcium hydroxide (CH) reduction in paste mixtures.

Findings

- Microspheres altered the air-void system. Mixtures with MS (particularly slurry-based MS [SM]) provided a better void distribution that enhanced strength and reduced secondary absorption. Their F/T performance was highly dependent on MS dispersion quality and consolidation method.
- Nanosilica increased the water-reducing admixture (WRA) demand in lab mixtures and reduced hardened air content relative to fresh air content but produced a finer air-void system with lower spacing factors, improving F/T resistance even when total air volume decreased.
- Mechanical properties of mixtures with MS were similar to or higher than those of the reference mixtures at all ages. Mixtures with nS did not reliably improve compressive strength but helped refine the microstructure of selected low w/c mixtures.
- Durability results showed that mixtures with MS reduced the secondary rate of water absorption and showed limited chloride ingress (but mostly at greater depths from the surface). Mixtures with nS showed small improvements in F/T testing despite higher w/c ratios. In contrast, mixtures containing both nS and MS underperformed in F/T resistance.
- Testing on paste mixtures confirmed that nS produced only slight reductions in CH content at all ages and w/c ratios. The amount of CH consumption varied slightly with the w/c ratio but remained mostly low. Compared to paste mixtures with Class C fly ash, nS showed a substantially lower pozzolanic activity.

Implementation

This project employed combined field trials, laboratory concrete testing, and paste evaluation to study the performance of MS and nS. Field slabs (8 × 8 ft) were cast using both traditional INDOT Class C mixture and mixtures modified with nS. Core samples were extracted at multiple ages for compressive strength, rate of water absorption, and chloride profile measurements following ASTM C39, ASTM C1585, and ASTM C1152, respectively. F/T resistance was evaluated using ASTM C666 in both field and lab specimens. Parameters of the air-void system were determined by ASTM C457, using manual counting for mixtures with MS, while automated counting was used for mixtures without MS. CH reduction was quantified using thermogravimetric analysis. These combined evaluations provide INDOT with a comprehensive understanding of how MS and nS influence durability performance under realistic variability in batching and construction conditions.

CONTENTS

1. INTRODUCTION . . . 10
   1.1 Background . . . 10
   1.2 Project Objectives . . . 10
2. MATERIALS AND TESTING PROCEDURE . . . 10
   2.1 Aggregates and Cement . . . 10
   2.2 Nanomaterials-Based Admixtures . . . 11
   2.3 Conventional and Alternative Air-Entraining Products . . . 11
   2.4 Water-Reducing Admixtures . . . 12
   2.5 Testing Procedure . . . 12
      2.5.1 Slump and Fresh Air Content . . . 12
      2.5.2 Parameters of the Air-Void System in Hardened Concrete . . . 12
      2.5.3 Compressive Strength . . . 12
      2.5.4 Flexural Strength . . . 12
      2.5.5 Rate of Water Absorption . . . 12
      2.5.6 Freeze-Thaw Resistance . . . 12
3. FIELD TRIALS OF CONCRETE MIXTURES WITH COLLOIDAL NANOSILICA AND ALTERNATIVE (MICROSPHERES) AIR-ENTRAINMENT PRODUCTS . . . 12
   3.1 Materials and Methods . . . 12
      3.1.1 Materials . . . 12
      3.1.2 Concrete Mixture Proportions and Mixing Methods . . . 12
      3.1.3 Testing Procedure . . . 13
   3.2 Field Trials and Collection of Cored Specimens . . . 13
   3.3 Discrepancies in the Amount of Water Used for Field Mixtures . . . 14
   3.4 Results and Discussions . . . 14
      3.4.1 Slump and Fresh Air Content . . . 14
      3.4.2 Parameters of the Air-Void System in Hardened Concrete . . . 15
      3.4.3 Compressive Strength . . . 16
      3.4.4 Flexural Strength . . . 17
      3.4.5 Rate of Water Absorption . . . 17
      3.4.6 Chloride Content Determination . . . 18
      3.4.7 Freeze-Thaw Resistance . . . 19
4. PRODUCTION OF LABORATORY SPECIMENS USING VARIABLE CONSOLIDATION METHODS TO ASSESS THE EFFECTS OF COLLOIDAL NANOSILICA AND MICROSPHERES ON THE FRESH, MECHANICAL, AND DURABILITY PROPERTIES OF CONCRETE . . . 20
   4.1 Materials and Methods . . . 20
      4.1.1 Materials . . . 20
      4.1.2 Concrete Mixture Design . . . 20
      4.1.3 Compaction Methods . . . 20
      4.1.4 Testing Procedures . . . 20
   4.2 Results and Discussions . . . 21
      4.2.1 Slump and Fresh Air Content . . . 21
      4.2.2 Parameters of the Air-Void System . . . 21
      4.2.3 Compressive Strength . . . 22
      4.2.4 Flexural Strength . . . 23
      4.2.5 Rate of Water Absorption . . . 23
      4.2.6 Freeze-Thaw Resistance . . . 23
5. QUANTIFICATION OF THE CALCIUM HYDROXIDE REDUCTION FOR PASTE MIXTURES WITH AND WITHOUT COLLOIDAL NANOSILICA . . . 25
   5.1 Materials and Methods . . . 25
      5.1.1 Materials . . . 25
      5.1.2 Testing Procedure . . . 25

5.2 Results and Discussions. 26
5.2.1 Quantification of Calcium Hydroxide Reduction 26

6. EFFECT OF COLLOIDAL NANOSILICA ON AIR-VOID SYSTEM AND POROSITY OF CONCRETES AS A FUNCTION OF THE WATER-TO-CEMENT RATIO 26
6.1 Materials and Methods 26
6.1.1 Materials 26
6.1.2 Concrete Mixture Design 26
6.1.3 Testing Procedures 26
6.2 Results and Discussions 27
6.2.1 Slump 27
6.2.2 Fresh and Hardened Air Content and Air-Void System Parameters 27
6.2.3 Compressive Strength 28
6.2.4 Initial and Secondary Absorption 28
6.2.5 Density, Absorption, and Voids in Hardened Concrete 29
6.2.6 Freeze-Thaw Resistance 29

7. CONCLUSIONS 30
7.1 Findings 30
7.1.1 Field Trials of Concrete Mixtures With Colloidal Nanosilica and Alternative (Microspheres) Air-Entrainment Products 30
7.1.2 Production of Laboratory Specimens Using Variable Consolidation Methods to Assess the Effects of Colloidal Nanosilica and Microspheres on the Fresh, Mechanical, and Durability Properties of Concrete 30
7.1.3 Quantification of the Calcium Hydroxide Reduction for Paste Mixtures With and Without Colloidal Nanosilica 31
7.1.4 Effect of Colloidal Nanosilica on Air-Void System and Porosity of Concretes as a Function of the Water-to-Cement Ratio 31
7.2 Recommendations and Future Work 31

REFERENCES 31

LIST OF TABLES

Table 2.1 Physical Properties of the Fine and Coarse Aggregates. 11

Table 2.2 Representative Chemical Composition of Cement. 11

Table 2.3 Solid Content and Dosage Rate of the nS Admixtures. 11

Table 3.1 CMDs in Saturated Surface-Dry (SSD) Conditions. 13

Table 3.2 Discrepancies in w/c Ratios Used for Field Mixtures. 14

Table 3.3 Slump and Fresh Air Content of All Mixtures. 14

Table 3.4 Characteristics of the Entrained Air in Hardened Concrete for the Reference Field Mixture. 15

Table 3.5 Characteristics of the Microsphere System for Field Mixtures. Observed at ~185x Magnification. 15

Table 3.6 Microsphere System Parameters for Assessment of Durability Potential of Concrete, Calculated Per Attiogbe (2022). 15

Table 4.1 CMDs in SSD Conditions. 20

Table 4.2 WRA Dosages, Slump, and Fresh Air Content Values. 21

Table 4.3 Characteristics of the Entrained Air in Hardened Concrete for the Reference Lab Mixture. 21

Table 4.4 Characteristics of the Microsphere System for Field Mixtures. Observed at ~185x Magnification. Observed at ~185x Magnification. 21

Table 4.5 Microsphere System Parameters for Assessment of Durability Potential of Concrete, Calculated Per (Attiogbe, 2022). 22

Table 5.1 Chemical Composition of Class C Fly Ash. 25

Table 6.1 CMDs in SSD Conditions. 27

Table 6.2 Air-Void System Parameters in Hardened Air Content. 28

Table 6.3 Summary of Absorption and Air-Void Space Characteristics. 29

LIST OF FIGURES

Figure 2.1 Gradation Curves of the Fine and Coarse Aggregates. 10

Figure 2.2 TEM Image of nS1. Figure courtesy of Dr. Raikhan Tokpatayeva. 11

Figure 2.3 TEM Image of nS2. Figure courtesy of Dr. Raikhan Tokpatayeva. 11

Figure 2.4 Optical Microscopy Image of the Appearance of CM With a Scale of 50 μm. 11

Figure 2.5 Optical Microscopy Image of the Appearance of SM With a Scale of 50 μm. 12

Figure 3.1 Schematic Layout of the Field Slabs Showing the Designated Coring and Ponding Areas. Courtesy of INDOT. NOTE: 1 ft = 0.3m. 14

Figure 3.2 Freshly Cast Concrete Slabs Immediately After Finishing. 14

Figure 3.3 Compressive Strength Results of Cast Cylinders. Data Courtesy of INDOT. NOTE: 1 psi = 0.007 MPa. 16

Figure 3.4 Compressive Strength Results of Cored Cylinders. Data Courtesy of INDOT. NOTE: 1 psi = 0.007 MPa. 16

Figure 3.5 Flexural Strength Results of All Mixtures. Data Courtesy of INDOT. NOTE: 1 psi = 0.007 MPa. 17

Figure 3.6 Initial Rate of Water Absorption of Cast Cylinders. 17

Figure 3.7 Secondary Rate of Water Absorption of Cast Cylinders. 17

Figure 3.8 Initial Rate of Water Absorption of Selected Cored Cylinders. 17

Figure 3.9 Secondary Rate of Water Absorption of Selected Cored Cylinders. 18

Figure 3.10 Chloride Content of Mixtures With 658 lb/cyd (390 kg/m^3) of Cement After 6 Months of Field Ponding. NOTE: 1 in. = 25.4 mm. 18

Figure 3.11 Chloride Content of Mixtures With and Without nS After 6 Months of Field Ponding. NOTE: 1 in. = 25.4 mm. 18

Figure 3.12 Chloride Content of Mixtures With 658 lb/cyd (390 kg/m^3) of Cement After 6 Months of Field Ponding and 6 Months of Lab Ponding. NOTE: 1 in. = 25.4 mm. 18

Figure 3.13 Chloride Content of Mixtures With and Without nS After 6 Months of Field Ponding and 6 Months of Lab Ponding. NOTE: 1 in. = 25.4 mm. 19

Figure 3.14 Freeze-Thaw Resistance of Mixtures With 658 lb/cyd of Cement (390 kg/m^3). 19

Figure 3.15 Freeze-Thaw Resistance of Mixtures With and Without nS. 19

Figure 4.1 Compressive Strength of All Mixtures at 7, 28, and 42 Days. NOTE: 1 psi = 0.007 MPa. 22

Figure 4.2 Flexural Strength of All Mixtures at 28 Days. NOTE: 1 psi = 0.007 MPa. 23

Figure 4.3 Initial Rate of Water Absorption for All Concrete Mixtures. 23

Figure 4.4 Secondary Rate of Water Absorption for All Concrete Mixtures. 23

Figure 4.5 Freeze-Thaw Resistance of All Concrete Mixtures Compacted Using a Rod. 24

Figure 4.6 Freeze-Thaw Resistance of C658 Mixtures With MS Using Both Compaction Methods. 24

Figure 4.7 Freeze-Thaw Resistance of C580-nS Mixtures With MS Using Both Compaction Methods. 25

Figure 5.1 CH Content Amount in Paste Mixtures at 7, 28, and 56 Days. 26

Figure 5.2 CH Consumed for Mixtures With nS Out of Available CH Based on the Respective Baseline Mixture. 26

Figure 6.1 Increase in WRA Dosages for Mixtures With nS With Respect to Their Respective Baseline Mixture. 27
Figure 6.2 Reduction in Fresh Air Content From Hardened Air Content. 27
Figure 6.3 Specific Surface of Hardened Air Void in All Mixtures. NOTE: 1 in.$^{-1}$ = 0.04 mm^{-1} 28
Figure 6.4 Compressive Strength of All Mixtures at 7 and 28 Days. NOTE: 1 psi = 0.007 MPa. 28
Figure 6.5 Initial Absorption for All Mixtures. NOTE: 1 mm = 0.04 in. 28
Figure 6.6 Secondary Absorption for All Mixtures. NOTE: 1 mm = 0.04 in. 29
Figure 6.7 Freeze-Thaw Resistance for All Mixtures. 30

1. INTRODUCTION

1.1 Background

The interest in the use of nanomaterials has increased in recent years due to their high surface area and reactivity. Among the most commonly researched nanomaterials are carbon-based materials (Shah et al., 2015) such as carbon nanotubes (Konsta-Gdoutos et al., 2010; Liew et al., 2016; Musso et al., 2009), carbon nanofibers (Meng & Khayat, 2018; Metaxa et al., 2013; Peyvandi et al., 2013), and nano graphene oxides (Maglad et al., 2022; Tong et al., 2016), as well as nano-titanium dioxide (Chen et al., 2012; Lee & Kurtis, 2010; Moro et al., 2021; Noorvand et al., 2013).

Nanosilica (nS) has specifically gained attention due to its ability to refine the pore structure of a composite as well as improve parameters such as strength or freeze-thaw (F/T) resistance (Huang et al., 2022; P. P. et al., 2021; Said et al., 2012; Singh et al., 2013). These improvements are largely attributed to the highly reactive amorphous silica that comprises nS. Its high specific surface area accelerates the consumption of calcium hydroxide (CH), which in turn promotes the formation of extra calcium silicate hydrate (CSH) gel (Björnström et al., 2004). The increased CSH production leads to a denser microstructure and strengthens the interfacial transition zone (ITZ), thus improving the bond between the cement paste and aggregates (Nili & Ehsani, 2015). However, careful attention should be placed on dispersing these materials, especially nS (Chuah et al., 2014; Kong et al., 2013). For this reason, nS suspended in a liquid medium (i.e., colloidal nS) has become increasingly preferred for practical applications.

Another potential concern with nS is its potential incompatibility with other admixtures, such as water-reducing admixtures (WRAs; Fernández et al., 2013) and air-entraining admixtures (AEAs; Yang et al., 2021). Microspheres (MS) may help address at least part of this issue, as they have been reported as an effective alternative to traditional AEAs for protecting concrete from F/T damage (Attiogbe, 2021). Specifically, MS coated in a powder blend and used at a dosage of 1% by volume in concrete mixtures have demonstrated adequate performance in terms of both compressive strength and F/T resistance (Attiogbe, 2022).

1.2 Project Objectives

The main objectives of the project were as follows:

- Conduct field trials and collect correct specimens for subsequent evaluations.
- Evaluate the effect of nS admixture and MS on the air-void characteristics of concretes developed for use in bridge decks.
- Compare the influence of concrete production (field vs. laboratory) on the durability and F/T performance of concrete.
- Assess the effect of mixing time, compaction efforts, and batching on the parameters of the air-void system and F/T resistance for field and lab concretes.
- Determine the impact of different water-to-cement (w/c) ratios on the mechanical and durability performance of concretes prepared with nS.

2. MATERIALS AND TESTING PROCEDURE

2.1 Aggregates and Cement

Natural siliceous sand conforming to Indiana Department of Transportation's (INDOT, 2024) Standard Specification Section 900 for No. 23 aggregate was used as the fine aggregate for this study. The coarse aggregate used was an 'AP' stone meeting the specifications for INDOT's Section 900 for No. 8 aggregate. Both aggregates were obtained from a ready-mix plant in Westfield, Indiana, to ensure consistency between the aggregates used in the field and those used in the lab. The gradation of both of these aggregates is shown in Figure 2.1. The physical properties of the aggregates can be seen in Table 2.1.

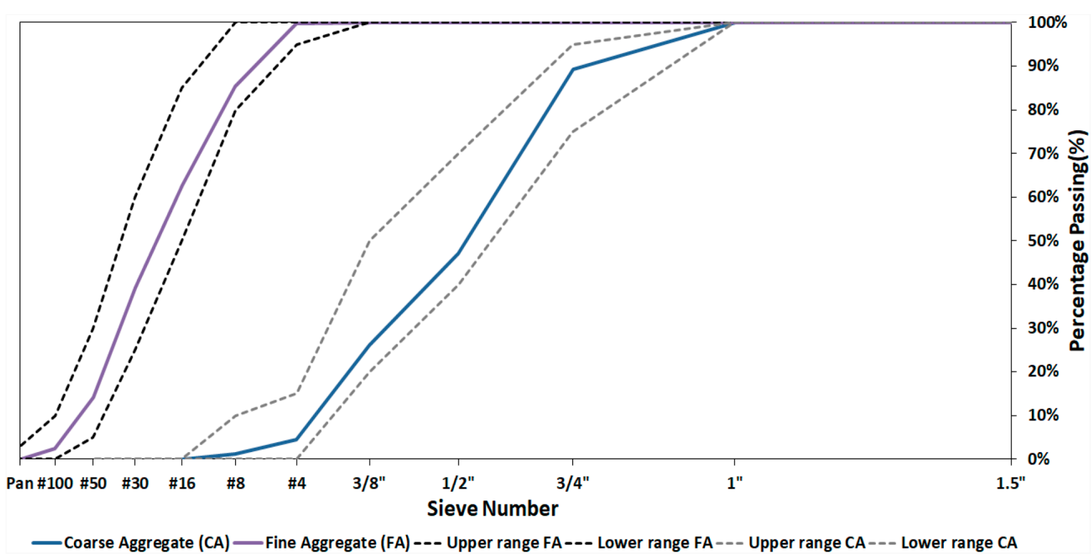

Figure 2.1 Gradation Curves of the Fine and Coarse Aggregates.

TABLE 2.1
Physical Properties of the Fine and Coarse Aggregates.

Aggregate	Saturated Surface-Dry (SSD) Specific Gravity	Absorption (%)
Fine Aggregate	2.65	1.49
Coarse Aggregate	2.62	3.12

TABLE 2.2
Representative Chemical Composition of Cement.

Composition	Wt. (%)
Al_2O_3	4.5
SiO_2	18.6
CaO	63.6
Fe_2O_3	2.4
MgO	2.6
SO_3	3.4
Limestone	11.0
Na_2O_{eq}	0.6

The cement used for this study consisted of Type IL cement following the specification of ASTM C595-24 (ASTM International [ASTM], 2024c). As multiple bags of cement were depleted throughout the study, a representative chemical composition of the cement can be seen in Table 2.2.

2.2 Nanomaterials-Based Admixtures

Two colloidal nanosilica (nS1 and nS2) admixtures were used at dosage rates recommended by suppliers and were always used simultaneously in all concrete mixtures. The main differences between nS1 and nS2 are their solid content and dosage rate, as observed in Table 2.3. Figure 2.2 and Figure 2.3 illustrate the appearance of both nS by using transmission electron microscopy (TEM), in which it can be observed that the average sizes are below 50 nm.

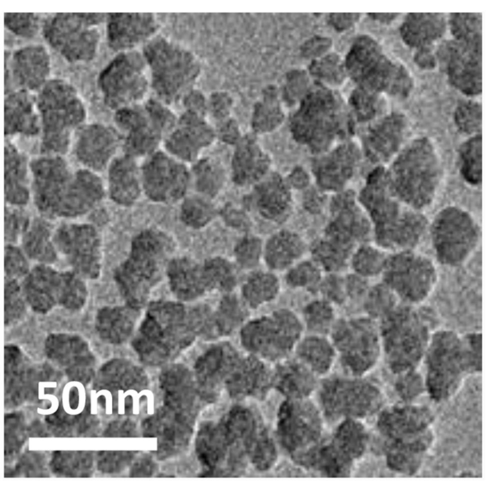

Figure 2.2 TEM Image of nS1. Figure courtesy of Dr. Raikhan Tokpatayeva.

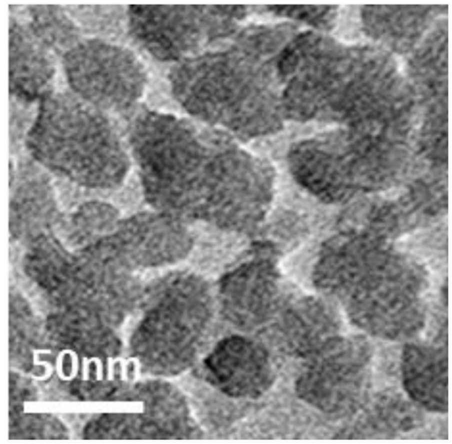

Figure 2.3 TEM Image of nS2. Figure courtesy of Dr. Raikhan Tokpatayeva.

TABLE 2.3
Solid Content and Dosage Rate of the nS Admixtures.

Colloidal Nanosilica Admixture	Water Content (%)	Solid Content (%)	Dosage rate (oz/cwt)
nS1	75.2	24.8	4.0
nS2	83.5	16.5	8.0

2.3 Conventional and Alternative Air-Entraining Products

The conventional AEA met the requirements of ASTM C260-24 (ASTM, 2024b). When used in concrete mixtures, it served as a benchmark for comparison against concrete mixtures with alternative air-entraining products, since they represent the type typically used in practice. Two different alternative air-entraining products, MS, were used. The first type consisted of polymeric MS coated with a mineral powder (Figure 2.4) to

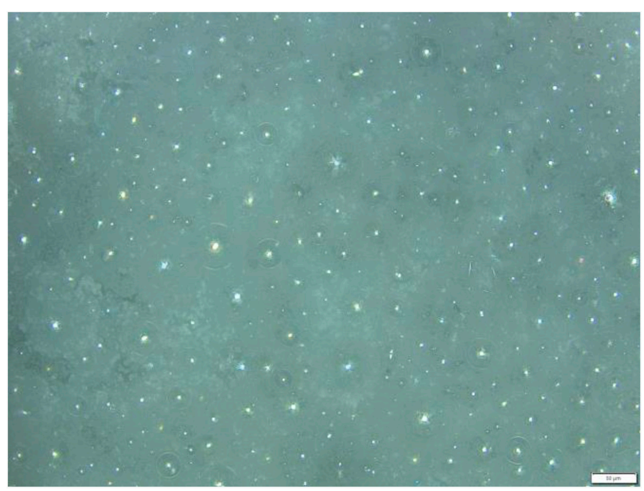

Figure 2.4 Optical Microscopy Image of the Appearance of CM With a Scale of 50 µm.

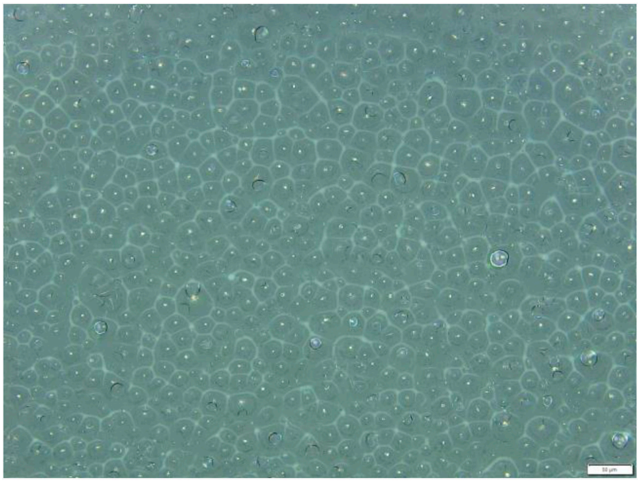

Figure 2.5 Optical Microscopy Image of the Appearance of SM With a Scale of 50 µm.

improve dispersion, while the second type consisted of polymeric MS dispersed in a slurry (Figure 2.5) for the same purpose. These are herein referred to as CM (coated microspheres) and SM (slurry-based microspheres).

2.4 Water-Reducing Admixtures

A WRA conforming to ASTM C494-24 (ASTM, 2024d) was used to meet the target slump values in lab mixtures. Field mixtures did not include the use of any WRAs.

2.5 Testing Procedure

To avoid repetition across the testing procedures used in each chapter, this section will encompass the common testing procedures that are used multiple times throughout this report. Additional details specific to each chapter's testing procedures are provided within the corresponding testing procedure sections of those chapters.

2.5.1 Slump and Fresh Air Content

Immediately after mixing, slump and air content measurements were made per ASTM C143-20 (ASTM, 2020d) and either ASTM C231-24 (pressure method; ASTM, 2024a) or ASTM C173-23 (volumetric method; ASTM, 2023), respectively.

2.5.2 Parameters of the Air-Void System in Hardened Concrete

The determination of the parameters of the air-void system in hardened concrete was determined following ASTM C457-24 (ASTM, 2024f) Method B ('Modified Point-Count Method') for concrete samples with MS and Method C ('Contrast Enhanced Method') for concrete samples without MS. Samples were cut perpendicular to the casting direction of the cylinders. The exposed surface was subsequently lapped and polished.

2.5.3 Compressive Strength

The compressive strength of cylinders was determined in accordance with ASTM C39-24 (ASTM, 2024e). Cylinders that were cast in molds were demolded after 24 hr and placed under lime-saturated water until their designated testing age.

2.5.4 Flexural Strength

Third-point load flexural strength was conducted on beams following ASTM C78-22 (ASTM, 2022b). Similar to the cylinders, the beams were cast and demolded after 24 hr and subsequently cured in lime-saturated water until their testing age.

2.5.5 Rate of Water Absorption

A modified version of ASTM C1585-20 (ASTM, 2020b) was used to determine the rate of water absorption. Two disks measuring 4 × 2 in. (102 × 51 mm) were cut from a 4 × 8 in. (102 × 203 mm) cylinder and were vacuum saturated at 28 days. For conditioning the specimens, they were placed in an oven at 60 °C (140 °F) until a constant mass was achieved.

2.5.6 Freeze-Thaw Resistance

To determine the F/T resistance, three beams were cast for each mixture and cured in lime-saturated water until the testing age, following ASTM C666-15 (ASTM, 2015), Procedure A. Approximately 35 cycles were completed over one week, with measurements taken at each of these 35 cycle intervals. The fundamental transverse frequency was determined according to ASTM E1876-22 (ASTM, 2022a) before the start of the experiment and after every 35 cycles. In addition, the relative dynamic modulus of elasticity (Pc) was calculated for each measurement taken.

3. FIELD TRIALS OF CONCRETE MIXTURES WITH COLLOIDAL NANOSILICA AND ALTERNATIVE (MICROSPHERES) AIR-ENTRAINMENT PRODUCTS

3.1 Materials and Methods

3.1.1 Materials

Details regarding the materials used in this chapter have previously been discussed in Chapter 2.

3.1.2 Concrete Mixture Proportions and Mixing Methods

The concrete mixture designs (CMDs) were developed by INDOT in accordance with Division 700, Section 702 of INDOT's 2022 Standard Specifications for structural concrete (INDOT, 2022), as seen in Table 3.1. For bridge deck applications, INDOT specifies the use of Class C concrete, which is a concrete composed of a cement content of 658 lb/cyd (390 kg/m^3), a maximum w/c ratio of 0.443, a minimum w/c ratio of 0.38, and a design air content of 6.5 ± 1.5% if traditional AEA is used. To evaluate the potential benefits of nS, alternative mixtures incorporating nS were developed for both field and laboratory conditions, with a

TABLE 3.1
CMDs in Saturated Surface-Dry (SSD) Conditions.

Mixture ID	Method of Mixing	Cement (lb/yd^3)	Water (lb/yd^3)	Fine Aggregate (lb/yd^3)	Coarse Aggregate (lb/yd^3)	Air-Entrainment Product	nS1 (oz/cwt)	nS2 (oz/cwt)
C658-W	Wet	658	289	1181	1645	Traditional	N/A	N/A
C658-SM-W	Wet	658	289	1252	1730	SM	N/A	N/A
C658-CM-W	Wet	658	289	1244	1730	CM	N/A	N/A
C658-SM-D	Dry	658	289	1252	1730	SM	N/A	N/A
C658-CM-D	Dry	658	289	1244	1730	CM	N/A	N/A
C580-NS-W	Wet	580	267	1242	1706	Traditional	4	8
C580-NS-SM-W	Wet	580	267	1310	1795	SM	4	8
C580-NS-CM-W	Wet	580	267	1294	1802	CM	4	8

NOTE: 1 lb/cyd = 0.593 kg/m^3, 1 oz/cwt = 65.2 mL/100kg.

reduced cement content of 580 lb/cyd (344 kg/m^3). These mixtures maintained a constant w/c ratio of 0.46 and the same target air content. When MS were incorporated, the target air content was set at 2.0%, consisting of entrapped air rather than intentionally entrained air. The nS and MS dosages, as well as the addition method, followed the supplier's recommendations.

In addition, two different methods of mixing and batching were followed: "wet" and "dry." The wet method of mixing consisted of mixing everything at the plant and placing the concrete in the truck, while the dry method of mixing consisted of placing and mixing everything in the truck. This was performed to evaluate what influence the mixing method would have on the performance of mixtures with MS.

3.1.3 Testing Procedure

3.1.3.1 Slump and Fresh Air Content. Details regarding procedures used for the determination of slump and fresh air content are presented in Chapter 2.

3.1.3.2 Parameters of the Air-Void System in Hardened Concrete. Details regarding procedures used for the determination of the parameters of the air void system in hardened concrete are presented in Chapter 2. Given that the recommended magnification to observe MS is 200x, performing Method B of ASTM C457 was impractical, as each sample can take up to 10 hr. Therefore, to evaluate the influence of compositional and batching parameters (i.e., "wet" or "dry" method of mixing), only the mixtures with a cement content of 658 lb/cyd (390 kg/m^3) were assessed. Additionally, only an area of 11 in.^{2} (71 cm^2) was used for the analysis.

3.1.3.3 Compressive Strength. Details about the determination of the compressive strength of the specimens are provided in Chapter 2. At each testing age (7 and 28 days), three 4 × 8 in. (102 × 204 mm) cylinders were tested in the lab. Cores from field mixtures, three 4 × 8 in. (102 × 204 mm) cylinders, were tested at 42 and 243 days.

3.1.3.4 Flexural Strength. For information regarding how flexural strength was conducted, please refer to Chapter 2. Beams measuring 6 × 6 × 21 in. (152 × 152 × 533 mm) were cast and remained in the field for the first 24 hr before being returned to the lab. Three beams were tested for each mixture at 28 days.

3.1.3.5 Rate of Water Absorption. For information regarding how the rate of water absorption was conducted, please refer to Chapter 2.

3.1.3.6 Chloride Content Determination. To determine the chloride content of cores extracted from the 4 × 4 ft (1.2 × 1.2 m) ponded area of the concrete slabs exposed to the 3% sodium chloride solution, ASTM C1152-20 (ASTM, 2020a) was followed. After the ponding period (about 6 months), three 2-in. (51 mm) diameter cores were extracted from each slab within the ponded region. Chloride content was then determined at four depths from the top surface of each core: 0.31, 0.88, 1.50, and 2.13 in. (8, 22, 38, and 54 mm).

To evaluate extended chloride ingress, two additional 4-in. diameter cores were extracted from the same ponded region and subjected to continuous ponding in the lab with the same type of solution (3% sodium chloride) for an additional 6 months. Five depths were used to assess chloride concentration for this extended exposure period: 0.50, 1.00, 1.50, 2.00, and 2.50 in. (13, 25, 38, 51, and 63 mm).

3.1.3.7 Freezing and Thaw Resistance. For information regarding how F/T resistance was conducted, please refer to Chapter 2. It should be noted that due to a temporary equipment malfunction, the beams (measuring 4 × 3 × 15.5 in. [102 × 76 × 394 mm]) cast in the field were kept frozen prior to testing, as permitted by the standard. Once the machine was operational, testing began.

3.2 Field Trials and Collection of Cored Specimens

The mixing and placement of concrete slabs were carried out during the summer outside of a commercial ready-mix plant in Indianapolis. The concrete was batched in a truck at the plant and transported to the placement area. Two slabs, each measuring 8 ft × 8 ft × 8 in. (2.4 × 2.4 × 0.2 m), were cast. One using a conventional Class C mixture, and the other using the modified

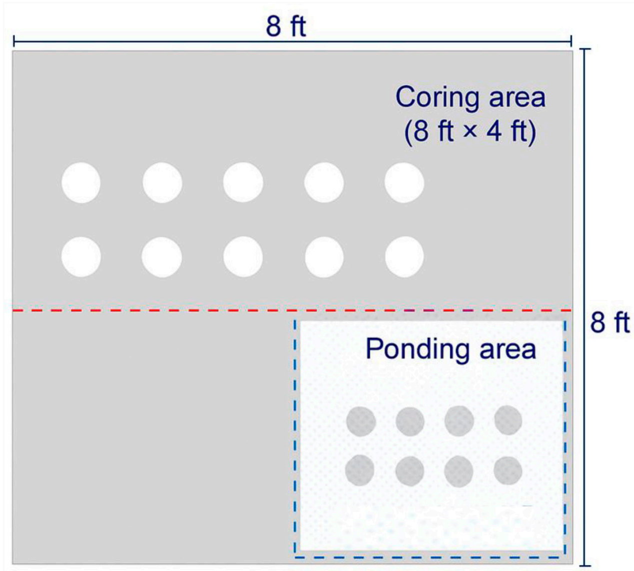

Figure 3.1 Schematic Layout of the Field Slabs Showing the Designated Coring and Ponding Areas. Courtesy of INDOT. NOTE: 1 ft = 0.3m.

Figure 3.2 Freshly Cast Concrete Slabs Immediately After Finishing.

CMD incorporating nS as previously mentioned. It is important to note that no external loads were applied to the slabs during the exposure period. Figure 3.1 shows a schematic of the layout of the slabs. The coring area (8 × 4 ft [2.4 × 1.2 m]), as observed in the schematic, indicates the region from which cores were extracted for compressive strength and rate of water absorption testing. The ponding area (4 ft × 4 ft [1.2 × 1.2 m]) represents the section of the slab that was exposed to continuous ponding with a 3% sodium chloride solution, beginning 60 days after the placement of the concrete slabs. A professional concrete finishing crew was hired to perform placement, compaction, and finishing. Curing was achieved by covering the slabs with plastic sheeting. Figure 3.2 shows the appearance of the slabs immediately after finishing. Cores were removed in accordance with ASTM C42-20 (ASTM, 2020c) to test for compressive strength (three per age), rate of water absorption (one), and chloride content determination (five per slab).

3.3 Discrepancies in the Amount of Water Used for Field Mixtures

After casting the concrete slabs, truck tickets with the batch ingredients were obtained, and discrepancies were observed in the w/c ratio used for each mixture, as summarized in Table 3.2. Specifically, the reported amount of water resulted in w/c ratios that were consistently lower than those specified in the intended mix designs. As such, the field trial results must be assessed carefully and with caution, since the exact w/c ratio of the concrete placed in the slabs and companion specimens is uncertain.

3.4 Results and Discussions

3.4.1 Slump and Fresh Air Content

The measured slump and fresh air content of all mixtures can be observed in Table 3.3. It should be noted that, given the discrepancies in the w/c ratio between all mixtures (Table 3.2), direct comparison of the performance may not be entirely suitable. All mixtures reached slump values of at least 4.00 in., indicating their suitability for bridge deck applications. In terms of the fresh air content, those using traditional AEA obtained air content values within the target air content, whereas those with MS, especially those with CM, obtained lower fresh air

TABLE 3.2
Discrepancies in w/c Ratios Used for Field Mixtures.

Mixture ID	w/c Ratio Per CMD	w/c Ratio Per Truck Ticket
C658-W		0.35
C658-SM-W		0.36
C658-CM-W	0.44	0.40
C658-SM-D		0.35
C658-CM-D		0.41
C580-NS-W		0.41
C580-NS-SM-W	0.46	0.36
C580-NS-CM-W		0.44

TABLE 3.3
Slump and Fresh Air Content of All Mixtures.

Mixture ID	Slump (in.)	Air Content (%)
C658-W	5.50	5.5 (pressure method)
C658-SM-W	4.75	4.3 (pressure method)
C658-CM-W	5.75	2.0 (volumetric method)
C658-SM-D	5.00	5.2 (pressure method)
C658-CM-D	5.00	2.0 (volumetric method)
C580-NS-W	6.50	7.0 (volumetric method)
C580-NS-SM-W	4.00	6.0 (volumetric method)
C580-NS-CM-W	6.50	1.75 (volumetric method)

NOTE: 1 in. = 25.4 mm.

contents. This lower fresh air content should be interpreted alongside the hardened air-void system parameters and the F/T resistance results to assess F/T risk properly. For CM mixtures, volumetric air content measurement is generally preferred over the pressure method. The pressure and volumetric methods were double-checked against one another to confirm that they produced consistent results.

3.4.2 Parameters of the Air-Void System in Hardened Concrete

A conventional AEA was used in the 658-W mixture, and thus, this mixture contained entrained air. From the results presented in Table 3.4, the C658-W mixture showed excellent air-void system parameters for F/T resistance. In particular, it had a spacing factor of 0.0015 in., well below the typical limit for F/T durability (0.008 in. [0.2 mm]). The specific surface area of the air voids in this mixture (934 in.$^{-1}$ [37 mm^{-1}]) also exceeded the threshold required for F/T durability (~600 in.$^{-1}$ [24 mm^{-1}]).

When evaluating the quality of the air-void system generated by the MS (again, using the criteria developed for concretes with conventional AEAs), it can be seen (see Table 3.5) that mixtures containing MS generally appear to provide a favorable void-system characteristics (spacing factor and specific surface) with respect to protection against F/T damage.

Table 3.5 also provides information on the characteristics of the microsphere system for field mixtures, which serves as an analog for air-void content. While the total microsphere content is relevant, other parameters such as microsphere frequency, average chord length, and specific surface are likely more critical due to the small size of the microspheres. Similar to entrained air-void systems, characteristics of the hardened microsphere system may provide more meaningful insight than the content alone. For example, two mixtures that appeared to have good potential for F/T resistance, C658-SM-W and C658-CM-D, had the lowest MS contents but exhibited a high frequency of MS, short chord lengths, and a specific surface of roughly 1600 in.$^{-1}$ (64 mm^{-1}; Table 3.5). In addition, these two mixtures had the lowest spacing factors, whether calculated using ASTM C457.

The C658-SM-D mixture had the highest MS content and total amount of MS, but its specific surface and spacing factor were not as favorable, although still within a range that may provide acceptable performance for F/T resistance. In contrast, the C658-CM-W mixture had the lowest overall MS content, frequency, and specific surface, along with a high spacing factor per ASTM C457. In other words, this mixture would be expected to perform the worst in terms of F/T resistance.

Table 3.6 presents the microsphere parameters for the assessment of the durability potential of concrete, calculated using the

TABLE 3.4
Characteristics of the Entrained Air in Hardened Concrete for the Reference Field Mixture.

Mixture ID	Hardened Air Content (%)	Void frequency (in.$^{-1}$)	Paste Content (%)	Avg. Chord Length (in.)	Specific Surface (in.$^{-1}$)	Spacing Factor (in.)
C658-W	3.9	9.3	30.0	0.005	934	0.0015

NOTE: 1 in.$^{-1}$ = 0.04 mm^{-1}, 1 in. = 25.4 mm.

TABLE 3.5
Characteristics of the Microsphere System for Field Mixtures. Observed at ~185x Magnification.

Mixture ID	MS Counted	MS Content (%)	MS frequency (in.$^{-1}$)	Avg. Chord Length (in.)	Specific Surface (in.$^{-1}$)	Spacing Factor Calculated per ASTM C457 (in.)
C658-SM-W	657	1.5	6.2	0.002	1642	0.004
C658-CM-W	479	2.1	4.6	0.005	871	0.01
C658-SM-D	1198	4.7	10.9	0.004	922	0.008
C658-CM-D	530	1.2	5.0	0.002	1630	0.006

NOTE: 1 in.$^{-1}$ = 0.04 mm^{-1}, 1 in. = 25.4 mm.

TABLE 3.6
Microsphere System Parameters for Assessment of Durability Potential of Concrete, Calculated Per Attiogbe (2022).

Mixture ID	Paste Content (%)	Spatial Distribution of MS, F	Dispersion Factor [Min. Limit Value]	Spacing Factor, $\bar{s}$ (in.)
C658-SM-W	25.7	0.44	24.8 [16.5]	0.002
C658-CM-W	26.4	0.59	18.3 [17.4]	0.004
C658-SM-D	26.2	1.22	43.44 [17.2]	0.004
C658-CM-D	29.4	0.32	20.17 [21.6]	0.003

NOTE: 1 in. = 25.4 mm.

literature formulas provided by (Attiogbe, 2022). For concrete to be considered durable, specifically in relation to F/T resistance, all three parameters (spatial distribution [F], dispersion factor, and spacing factor [$\bar{s}$]) must satisfy their respective criteria. Specifically, F must be equal to or greater than 0.27, the dispersion factor must be equal to or greater than 10 times the paste content by volume, and $\bar{s}$ must be equal to or smaller than 0.008 in. (0.2 mm).

The results presented in Table 3.6 are consistent with the microsphere system characteristics shown in Table 3.5, indicating good potential for F/T resistance in mixtures C658-SM-W, C658-CM-W, and C658-SM-D, as all three meet the required criteria for each parameter simultaneously. In contrast, the C658-CM-D mixture may not be entirely suitable with respect to F/T resistance, as its dispersion factor falls below the minimum limit value. Overall, mixtures with slurry microspheres (SM) tended to develop a more favorable air-void system than those with CM, as only one CM mixture (C658-CM-W) showed clearly adequate characteristics.

3.4.3 Compressive Strength

The compressive strength results for cast cylinder mixtures are shown in Figure 3.3. At 7 days, all C658 mixtures achieved strengths of at least 4500 psi (31 MPa), and at 28 days they reached a minimum of 5200 psi (36 MPa). It should be noted that, despite having a similar or higher w/c ratios, the mixtures with MS performed similarly or better than the reference C658 mixture at both ages. This suggests that mixtures with MS increase the compressive strength of concrete. For mixtures with nS, similar trends can be observed, where mixtures with MS perform comparably to or better than the reference nS mixture at this lower cement content.

The compressive strength of the cores at 42 and 243 days can be seen in Figure 3.4. Similar to before, the mixtures with MS perform comparably to or better than their corresponding reference mixture (either plain cement or with nS) at all ages. Mixtures with CM, which were inadvertently batched at a higher w/c ratio, produced the highest strengths at all ages for any group.

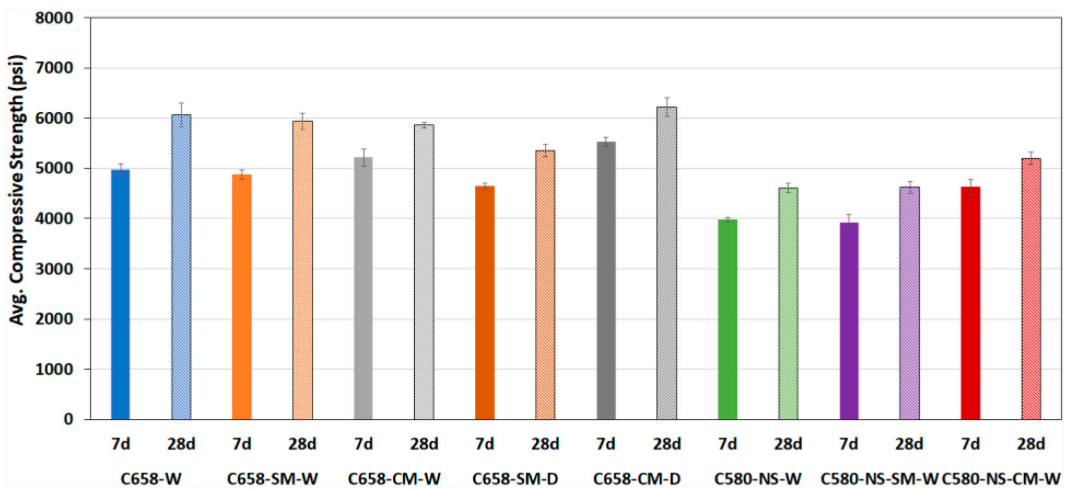

Figure 3.3 Compressive Strength Results of Cast Cylinders. Data Courtesy of INDOT. NOTE: 1 psi = 0.007 MPa.

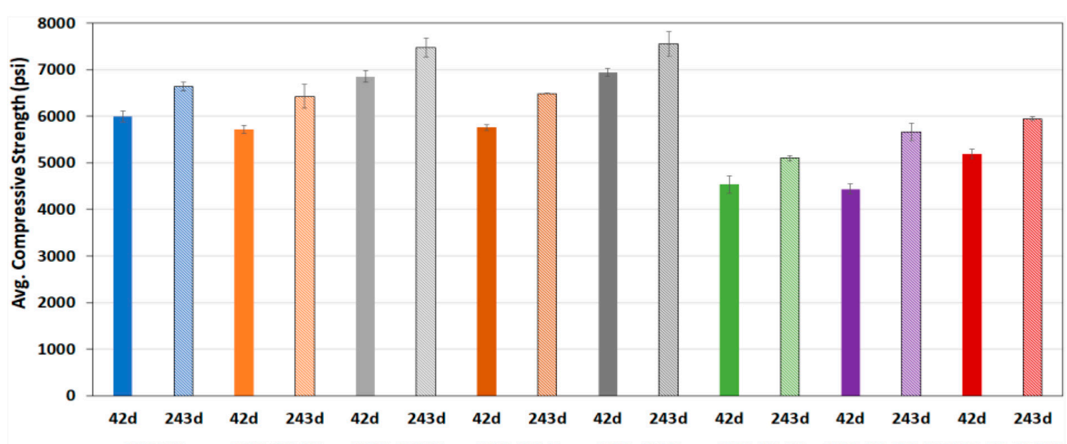

Figure 3.4 Compressive Strength Results of Cored Cylinders. Data Courtesy of INDOT. NOTE: 1 psi = 0.007 MPa.

3.4.4 Flexural Strength

The 28-day flexural strength results for all concrete mixtures are presented in Figure 3.5. The C658 mixtures performed similarly, each obtaining flexural strengths of at least 670 psi (4.6 MPa), with C658-CM-D showing the highest value within this cement content. When nS was incorporated, mixtures containing CM again showed the highest flexural strengths, similar to the trends observed in the compressive strength results. It is also worth noting that the MS mixtures with nS showed flexural strengths comparable to their counterparts containing only MS.

3.4.5 Rate of Water Absorption

The initial rate of water absorption results can be observed in Figure 3.6. As the underlying mechanism that controls the initial rate of water absorption in concrete specimens is capillary porosity, the w/c ratio significantly influences the rate of water absorption in the first 6 hr. For the C658 mixtures, the "wet" mixing method appeared to provide improved results over the "dry" method when MS were used. Furthermore, despite the higher w/c ratio, C658-SM-W and C658-CM-W both showed a lower initial rate of water absorption than the C658-W mixture. At a lower cement content but higher w/c ratio, the reference mixture with nS (C580-NS-W) performed similarly to the plain reference mixture (C658-W), showcasing the benefits of nS on this particular mixture. However, the performance of mixtures with nS and MS was worse than the reference mixture with nS when taking the w/c ratio into account.

The results from the secondary rate of water absorption are presented in Figure 3.7. Secondary rate of water absorption is largely governed by the air-void system in the specimens, which explains why mixtures with MS had a lower secondary rate of water absorption than their respective reference mixture (either plain cement or with nS). The method of mixing when MS were included appeared to play a smaller role for SM mixtures than for the CM mixtures, in which the "dry" method of mixture appeared to be desirable for the latter.

To verify the expected performance of the slabs based on the cast cylinders, cores were extracted and tested for the initial (Figure 3.8) and secondary (Figure 3.9) rate of water absorption. The selected mixtures demonstrated a similarity

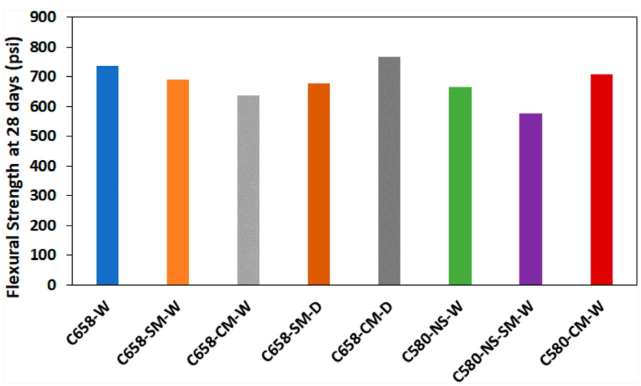

Figure 3.5 Flexural Strength Results of All Mixtures. Data Courtesy of INDOT. NOTE: 1 psi = 0.007 MPa.

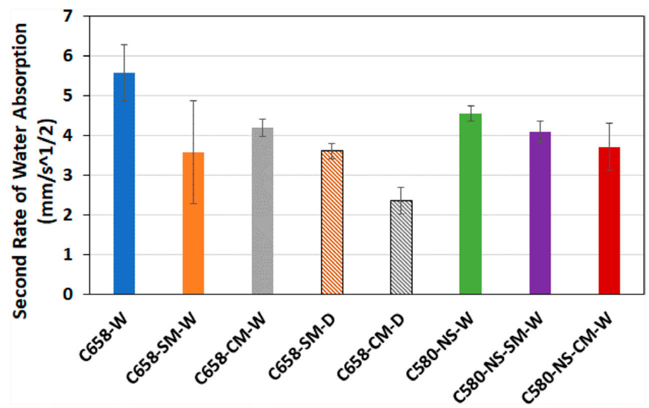

Figure 3.7 Secondary Rate of Water Absorption of Cast Cylinders.

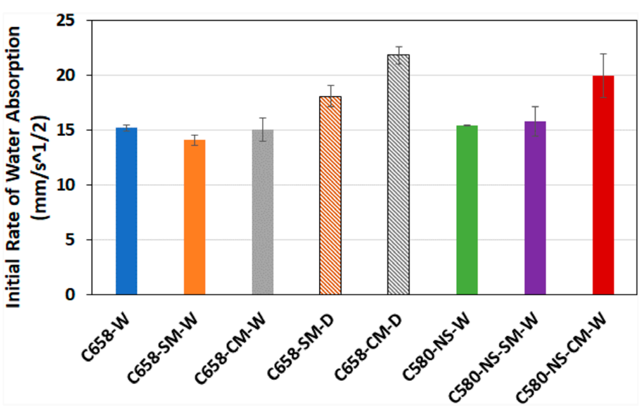

Figure 3.6 Initial Rate of Water Absorption of Cast Cylinders.

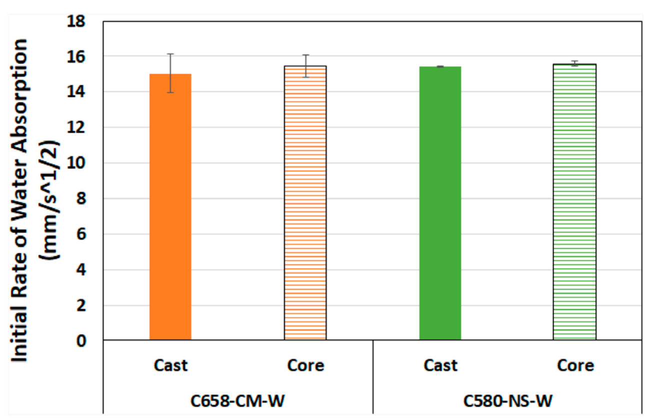

Figure 3.8 Initial Rate of Water Absorption of Selected Cored Cylinders.

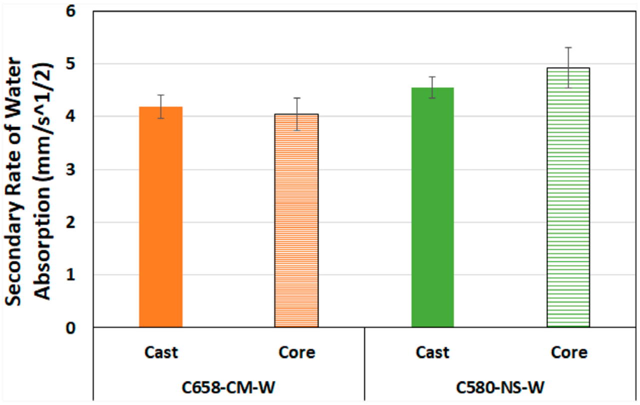

Figure 3.9 Secondary Rate of Water Absorption of Selected Cored Cylinders.

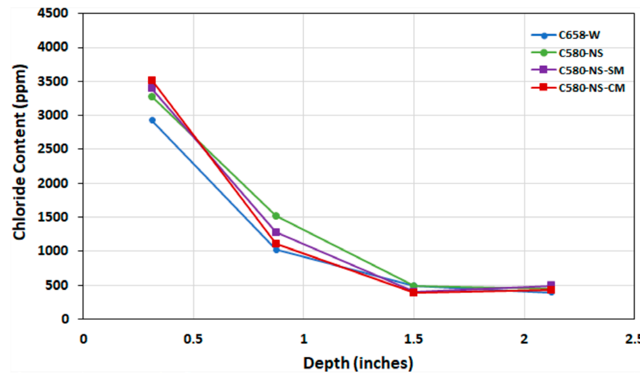

Figure 3.11 Chloride Content of Mixtures With and Without nS After 6 Months of Field Ponding. NOTE: 1 in. = 25.4 mm.

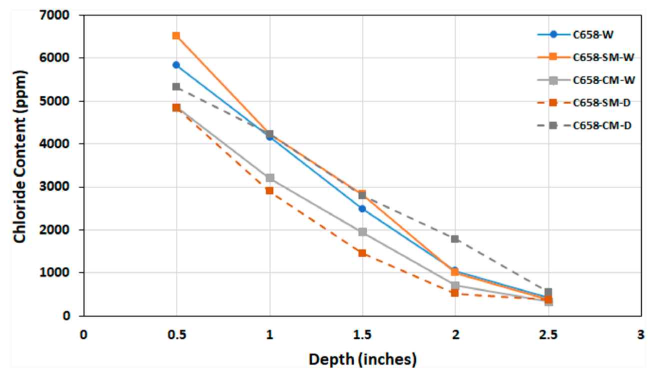

Figure 3.12 Chloride Content of Mixtures With 658 lb/cyd (390 kg/m^3) of Cement After 6 Months of Field Ponding and 6 Months of Lab Ponding. NOTE: 1 in. = 25.4 mm.

between cast cylinders and cored samples, indicating an agreement in results across the specimens. The largest deviation was observed for the C580-NS-W mixture in the secondary rate of water absorption results, where cores produced a relatively low increase of about 8% compared to the cylinders. This suggests that the performance of field slabs, at least in terms of rate of water absorption, can be fairly assessed by the cast cylinders.

3.4.6 Chloride Content Determination

For the mixtures exposed to 6 months of ponding in the field and with 658 lb/cyd (390 kg/m^3) of cement (Figure 3.10), the use of MS, with the exception of C658-SM-D, appeared to result in a higher chloride content at a depth of 0.31 in. (8 mm), by about 700 ppm. At greater depths, the results of the mixtures were comparable to one another.

For the mixtures with nS and lower (580 lb/cyd) cement content, the chloride contents were also higher than those of the plain reference mixture, as seen in Figure 3.11. However, incorporating MS in these nS mixtures led to comparable or improved performance, particularly at 0.88 in. (22 mm), than the reference mixture with nS. However, it should be noted that the w/c ratio varied among all mixtures, which likely contributed to some of these differences.

The results from the extended ponding (i.e., 6 months in the field followed by 6 months in the lab) generally demonstrated favorable performance for the C658 mixtures with MS compared to the plain reference mixture. Specifically, at a depth of 0.5 in. (13 mm), mixtures with MS (with the exception of C658-SM-W) had approximately 500–1000 ppm lower chloride contents. With increasing depth, both types of MS mixtures performed better than the plain reference mixture (depending on the method of mixing), and mixtures incorporating the same MS type but different mixing methods showed a comparable performance.

For the mixtures with nS, all mixtures now performed comparably to or better than their plain reference mixtures (Figure 3.12). Analyzing the effect of MS in the nS mixtures (Figure 3.13), the mixtures with MS and nS performed better than or similar to the nS reference mixture at all depths. However, it should again be noted that the w/c ratio was different among all mixtures, which likely influenced the chloride content results.

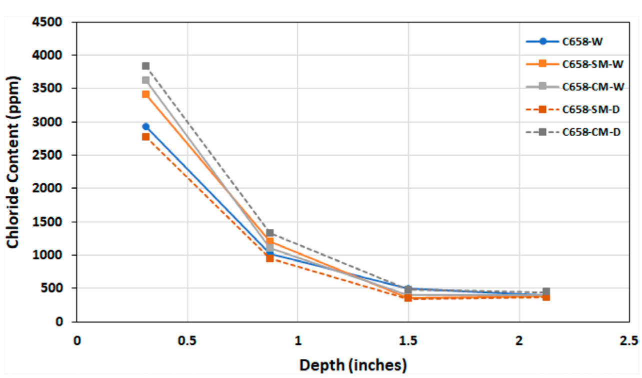

Figure 3.10 Chloride Content of Mixtures With 658 lb/cyd (390 kg/m^3) of Cement After 6 Months of Field Ponding. NOTE: 1 in. = 25.4 mm.

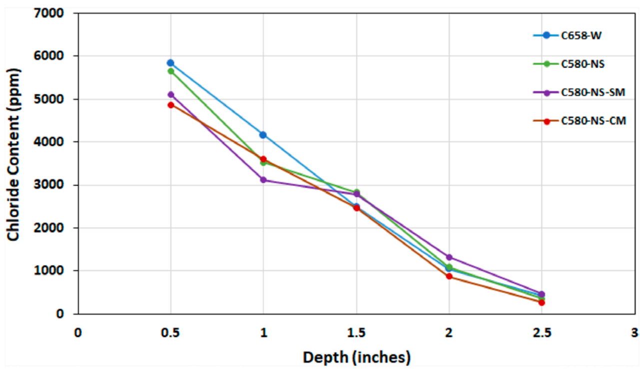

Figure 3.13 Chloride Content of Mixtures With and Without nS After 6 Months of Field Ponding and 6 Months of Lab Ponding. NOTE: 1 in. = 25.4 mm.

3.4.7 Freeze-Thaw Resistance

Specimens were subjected to approximately 330 F/T cycles. For the C658 mixtures (Figure 3.14), all mixtures, with the exception of C658-CM-W, met the minimum requirement of achieving at least 60% of the relative elastic modulus (Pc) at the end of the experiment. The best performing mixture was C658-SM-W, which showed a significantly better performance than the plain reference mixture, both of which had a comparable w/c ratio. Because the w/c ratios were similar within each MS across each mixing methods (e.g., C658-SM-W vs. C658-SM-D and C658-CM-W vs. C658-CM-D), these results suggest that, in terms of F/T resistance, the "dry" mixing method is more beneficial for CM mixtures (as also observed in the secondary rate of water absorption measurements), whereas the "wet" mixing

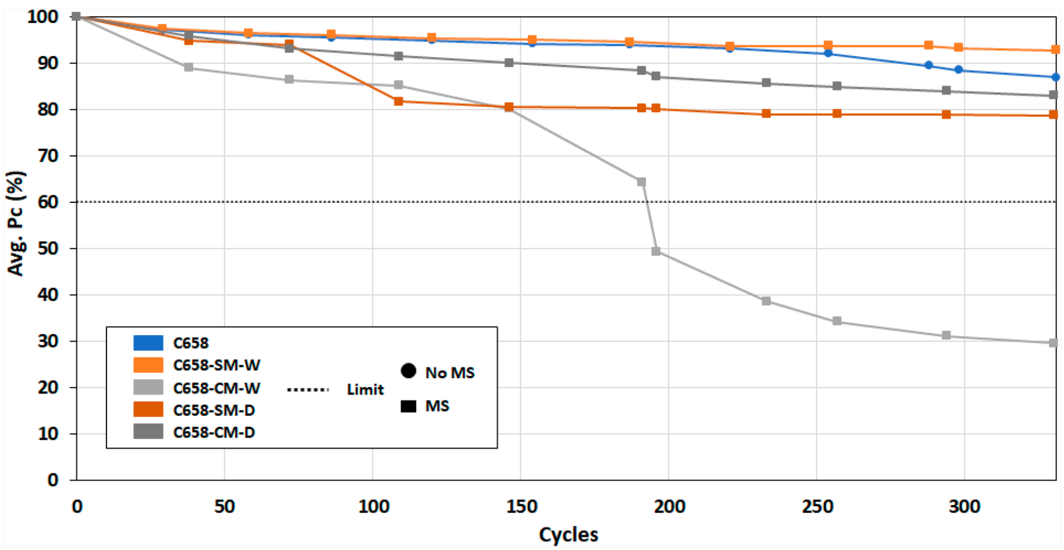

Figure 3.14 Freeze-Thaw Resistance of Mixtures With 658 lb/cyd of Cement (390 kg/m³).

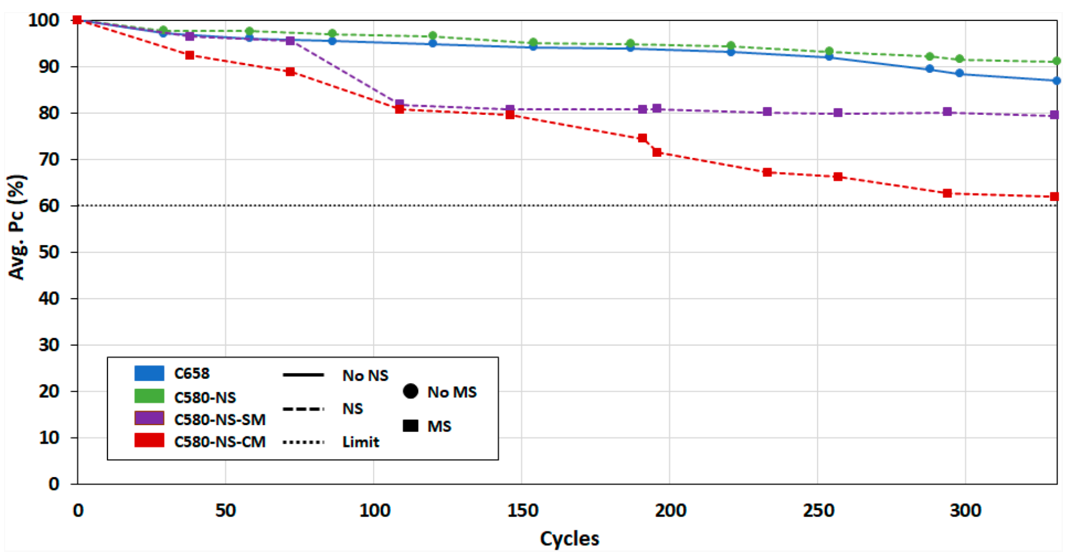

Figure 3.15 Freeze-Thaw Resistance of Mixtures With and Without nS.

method provides further improvements for the SM mixtures. In addition, these results are in agreement with those obtained from the parameters of the air-void system, in which C658-SM-W had the best potential for F/T protection while C658-CM-W had the worst potential.

Figure 3.15 presents the F/T resistance results of mixtures with and without nS. It can be seen that the reference mixture with nS achieved a higher Pc than the plain reference mixture, despite having a higher w/c ratio. In contrast, containing both nS and MS performed considerably worse than either reference mixture, but still obtained a Pc of at least 60%. Similar to the C658 mixtures, those incorporating SM showed better performance than the corresponding CM mixtures.

4. PRODUCTION OF LABORATORY SPECIMENS USING VARIABLE CONSOLIDATION METHODS TO ASSESS THE EFFECTS OF COLLOIDAL NANOSILICA AND MICROSPHERES ON THE FRESH, MECHANICAL, AND DURABILITY PROPERTIES OF CONCRETE

4.1 Materials and Methods

4.1.1 Materials

Details regarding the materials used in this chapter have previously been discussed in Chapter 2.

4.1.2 Concrete Mixture Design

The CMDs were closely developed to resemble those used in the field trials (Chapter 3), to accurately assess the performance of lab mixtures in comparison to field mixtures. However, as the batch water in the field mixtures varied, a comparative performance between lab and field mixtures is inadequate. Only the "wet" mixing method was followed for lab mixtures. In total, six CMDs—C658 mixtures with and without MS and C580 mixtures with nS and with and without MS—were adopted from the field and used in the lab, while one CMD (C580 plain reference) was introduced to serve as a baseline for the mixtures with a cement content of 580 lb/cyd (344 kg/m^3). Mixtures with a cement content of 658 lb/cyd (390 kg/m^3) of cement were still designed with a w/c ratio of 0.44, while those with the lower cement content of 580 lb/cyd (344 kg/m^3) had a w/c ratio of 0.46. All mixtures required the use of WRA to achieve a target slump of at least 3.00 in. (76 mm), while those without MS required the use of traditional AEA to meet the air content of 6.5% ± 1.5%. Table 4.1 provides a summary of all CMDs used.

4.1.3 Compaction Methods

To evaluate the compaction efforts on the characteristics of the air-void system and F/T resistance, those with MS were cast using two different compaction methods, following ASTM C192: rodding and vibrating. All other mixtures were compacted using a rod.

4.1.4 Testing Procedures

4.1.4.1 Slump and Fresh Air Content. Details regarding procedures used for the determination of slump and fresh air content are presented in Chapter 2.

4.1.4.2 Parameters of the Air-Void System in Hardened Concrete. Details regarding procedures used for the determination of the parameters of the air-void system in hardened concrete are presented in Chapter 2. Given that determining the parameters of the air-void system was impractical (i.e., each sample taking up to 10 hr), and that field mixtures with a cement content of 658 lb/cyd (390 kg/m^3) were previously assessed, those with a cement content of 580 lb/cyd (344 kg/m^3) were studied to understand the effect of consolidation. Furthermore, only an area of 11 in.^{2} (71 cm^2) was used for the analysis.

4.1.4.3 Compressive Strength. Details about the determination of the compressive strength of the specimens are provided in Chapter 2. At each testing age (7, 28, and 42 days), three 4 × 8 in. (102 × 204 mm) cylinders were tested in the lab.

4.1.4.4 Flexural Strength. For information regarding how flexural strength was conducted, please refer to Chapter 2. Three beams measuring 4 × 4 × 14 in. (102 × 102 × 356 mm) were tested for each mixture at 28 days.

4.1.4.5 Rate of Water Absorption. For information regarding how the rate of water absorption was conducted, please refer to Chapter 2.

TABLE 4.1
CMDs in SSD Conditions.

Mixture ID	Cement (lb/yd^3)	Water (lb/yd^3)	Fine Aggregate (lb/yd^3)	Coarse Aggregate (lb/yd^3)	Air-Entrainment Product	nS1 (oz/cwt)	nS2 (oz/cwt)
C658	658	289	1178	1644	Traditional	N/A	N/A
C658-SM	658	289	1254	1732	SM	N/A	N/A
C658-CM	658	289	1246	1723	CM	N/A	N/A
C580	580	267	1242	1704	Traditional	N/A	N/A
C580-nS	580	267	1242	1704	Traditional	4	8
C580-nS-SM	580	267	1313	1798	SM	4	8
C580-nS-CM	580	267	1293	1801	CM	4	8

NOTE: 1 lb/cyd = 0.593 kg/m^3, 1 oz/cwt = 65.2 mL/100kg.

4.1.4.6 Freezing and Thaw Resistance. For information regarding how F/T resistance was conducted, please refer to Chapter 2. It should be noted that due to a temporary equipment malfunction, the beams (measuring 4 × 3 × 15.5 in. [102 × 76 × 394 mm]) cast in the field were kept frozen prior to testing, as permitted by the standard. Once the machine was operational, testing began.

4.2 Results and Discussions

4.2.1 Slump and Fresh Air Content

The WRA dosages, slump, and fresh air content of all mixtures are summarized in Table 4.2. As observed, all mixtures with a higher cement content required a lower dosage of WRA with respect to the C580 mixtures, despite having a slightly lower w/c ratio. This can be explained by the considerably higher cement content in these mixtures (78 lb [35 kg] extra), which aids in terms of workability and thus outweighs the effects of the slight difference in w/c ratio. For either type of mixture (C658 or C580), the use of MS considerably increased the use of WRA to achieve the target slump. Similarly, nS further reduced the workability of these mixtures. In terms of MS, mixtures with CM appeared to increase the dosage of WRA in comparison to the SM mixtures, given that they are not dispersed in a "slurry" form. In terms of air content, similarly to field mixtures, both pressure and volumetric methods produced similar results.

4.2.2 Parameters of the Air-Void System

The C580-nS mixture was the only mixture containing entrained air, as it was produced using a conventional AEA. As shown in Table 4.3, the hardened concrete prepared using C580-nS mixture developed a desirable air-void system, characterized by a high specific surface area of the air voids (1925 in.$^{-1}$ [77 mm^{-1}]) and a spacing factor of 0.002 in. (0.05 mm), well below the commonly accepted limit of 0.008 in. (0.2 mm). These characteristics indicate a strong potential for resistance to F/T damage.

The influence of compaction effort (i.e., rodding or vibration) on the characteristics of the MS system in hardened concrete is summarized in Table 4.4. For the SM mixtures, it was observed that the compaction effort had a considerable impact. Specifically, vibrating the mixtures produced better microsphere system characteristics than rodding. When vibrating

TABLE 4.2
WRA Dosages, Slump, and Fresh Air Content Values.

Mixture ID	WRA dosage (oz/cwt)	Slump (in.)	Air Content (pressure method, %)	Air Content (volumetric method, %)
C658	1.5	3.00	6.4	6.0
C658-SM	2.6	4.50	3.8	3.0
C658-CM	3.1	3.50	2.6	2.25
C580	4.3	3.00	5.4	N/A
C580-nS	5.7	3.00	6.9	6.25
C580-nS-SM	6.1	3.00	3.1	3.25
C580-nS-CM	6.7	3.00	2.3	1.75

NOTE: 1 oz/cwt = 65.2 mL/100kg, 1 in. = 25.4 mm.

TABLE 4.3
Characteristics of the Entrained Air in Hardened Concrete for the Reference Lab Mixture.

Mixture ID	Hardened Air Content (%)	Void Frequency (in.$^{-1}$)	Paste Content (%)	Avg. Chord Length (in.)	Specific Surface (in.$^{-1}$)	Spacing Factor (in.)
C580-nS	5.9	17.6	28.0	0.002	1925	0.002

NOTE: 1 in.$^{-1}$ = 0.04 mm^{-1}, 1 in. = 25.4 mm.

TABLE 4.4
Characteristics of the Microsphere System for Field Mixtures. Observed at ~185x Magnification.

Mixture ID	MS Counted	MS Content (%)	MS Frequency (in.$^{-1}$)	Specific Surface (in.$^{-1}$)	Spacing Factor Calculated Per ASTM C457 (in.)
C580-nS-SM-ROD	236	1.1	2.1	787	0.01
C580-nS-SM-VIB	493	1.0	4.1	1643	0.009
C580-nS-CM-ROD	372	0.8	3.4	1653	0.007
C580-nS-CM-VIB	429	0.9	3.7	1560	0.004

NOTE: 1 in.$^{-1}$ = 0.04 mm^{-1}, 1 in. = 25.4 mm.

TABLE 4.5
Microsphere System Parameters for Assessment of Durability Potential of Concrete, Calculated Per (Attiogbe, 2022).

Mixture ID	Paste Content (%)	Spatial Distribution of MS, F	Dispersion Factor [Min. Limit Value]	Spacing Factor, s̄ (in.)
C580-nS-SM-ROD	28.5	0.29	8.4 [20.3]	0.006
C580-nS-SM-VIB	28.2	0.27	16.3 [19.8]	0.003
C580-nS-CM-ROD	27.8	0.23	13.7 [19.3]	0.002
C580-nS-CM-VIB	28.2	0.26	16.7 [19.9]	0.003

NOTE: 1 in. = 25.4 mm.

these mixtures, their frequency and specific surface increased relative to the mixtures that were rodded. The spacing factor calculated using ASTM C457 was above the typical threshold.

For the CM mixtures, a similar trend was observed where vibration improved the characteristics of the MS system by yielding slightly higher MS frequency and total MS count. Overall, at this lower cement content with nS, neither compaction method consistently achieved desirable parameters for F/T resistance, but vibration clearly moved both SM and CM mixtures closer to the desired MS system characteristics.

Table 4.5 demonstrates the MS system parameters for the assessment of the durability of concrete. The influence of compaction effort on the microsphere system is clearly reflected in three key parameters, F, dispersion factor, and s̄, which quantify how effectively the microspheres are distributed throughout the system. These parameters are particularly important, as meeting their respective threshold values indicates that the microspheres are well dispersed and not prone to agglomeration. When SM mixtures were vibrated, a higher dispersion was obtained in comparison with when rodding was used as the compaction method. However, this dispersion factor still did not reach the minimum threshold required to be classified as well dispersed. Both F and s̄ were calculated using the literature equations (Attiogbe, 2022) and met the typical threshold values (F must be equal to or greater than 0.27, and s̄ must be equal to or smaller than 0.008 in [0.2 mm]). However, because the dispersion factor did not meet the target criteria (equal to or greater than 10 times the paste content by volume), these variables alone may not fully represent the expected F/T performance.

For the CM mixtures, a similar trend was observed, with vibration improving dispersion by having both the dispersion factor and F values approaching the minimum limits. However, for both CM mixtures, F still remained below the threshold, even though the s̄ criteria were satisfied. Overall, these mixtures performed worse than the SM mixtures, and their F/T performance is therefore expected to be limited, although vibration provided a noticeable improvement. Among all mixtures evaluated, the C580-nS-SM-VIB mixture appears to have the greatest potential to show adequate F/T resistance.

4.2.3 Compressive Strength

The compressive strength of all mixtures is seen in Figure 4.1. As presented, for C658 mixtures, those with MS obtained considerably higher strengths than the reference

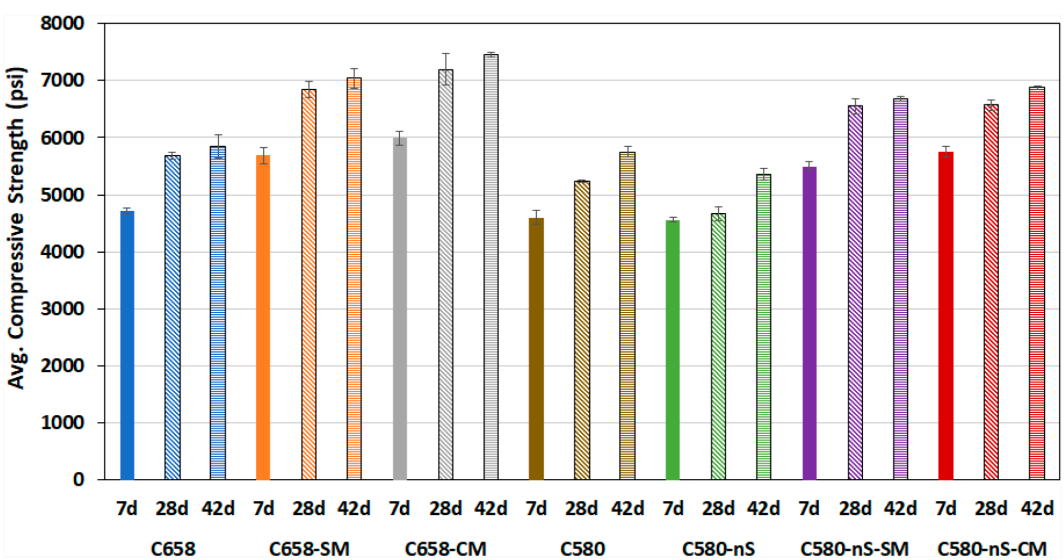

Figure 4.1 Compressive Strength of All Mixtures at 7, 28, and 42 Days. NOTE: 1 psi = 0.007 MPa.

mixture at all ages. Specifically, at 7 days, mixtures with MS obtained strengths similar to or better than the reference mixture at 42 days. It should also be noted that those mixtures with CM performed the best. In terms of C580 mixtures, it was evident that the addition of nS did not improve the strength compared to the plain reference mixture. However, the use of MS improved the performance of the C580 mixtures with nS, as previously observed for the C658 mixtures. Similar trends prevailed, where the 7-day strength of these mixtures with MS was higher than the plain mixture with nS at 42. Mixtures with CM also appeared to perform the best.

4.2.4 Flexural Strength

All mixtures performed comparatively to one another, with C658 mixtures having slightly higher flexural strengths (Figure 4.2). All mixtures obtained a flexural strength of at least 1000 psi (6.9 MPa). Mixtures with CM showed the highest overall strength. The addition of nS did not produce any noticeable effects in comparison to the plain reference mixture.

4.2.5 Rate of Water Absorption

The initial rate of water absorption showcased a similar performance in the C658 mixtures with or without MS, as seen in Figure 4.3. For C580 mixtures, those containing nS had a higher initial rate of water absorption compared to the plain reference mixture, demonstrating a worse performance. When mixtures contained both nS and MS, similarly to C658 mixtures, they performed comparably to the baseline mixture with nS.

The secondary rate of water absorption demonstrated different trends from those observed for the initial rate of water absorption. As seen in Figure 4.4, in the C658 mixtures, those with MS had a lower secondary rate of water absorption. Since this parameter is controlled by the air-void system in the mixtures, those with MS had a superior performance since they have a lower hardened air-void content. For the C580 mixtures, those containing nS performed similarly to the plain reference mixture. When mixtures contained both nS and MS, the secondary rate of water absorption was further lowered, demonstrating an improved performance. For either type of cement mixtures, both SM and CM had comparable results.

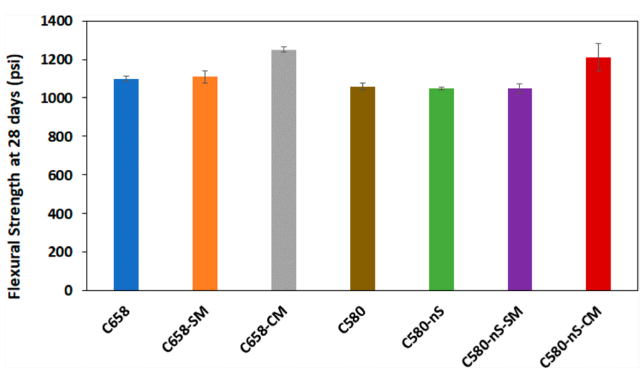

Figure 4.2 Flexural Strength of All Mixtures at 28 Days.
NOTE: 1 psi = 0.007 MPa.

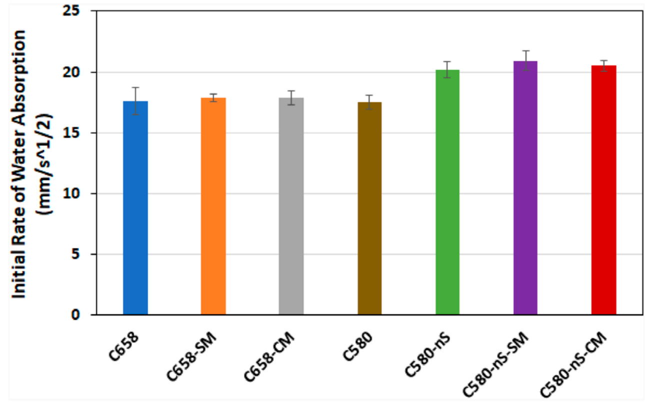

Figure 4.3 Initial Rate of Water Absorption for All Concrete Mixtures.

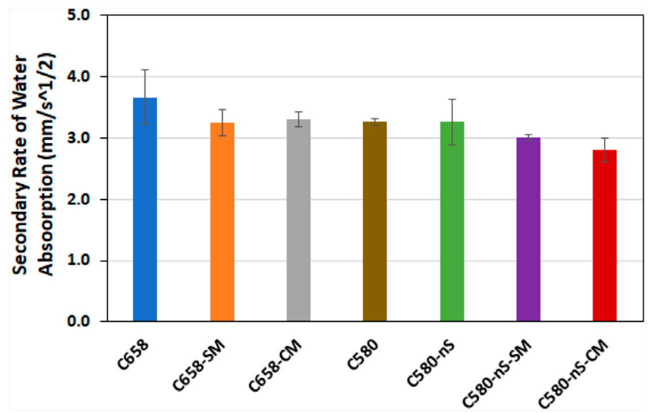

Figure 4.4 Secondary Rate of Water Absorption for All Concrete Mixtures.

4.2.6 Freeze-Thaw Resistance

The F/T resistance of all mixtures that were compacted with a rod can be found in Figure 4.5. For the C658 mixtures, the reference mixture performed particularly well with a Pc of about 87% at around 300 cycles. However, those containing MS did not meet the minimum established threshold by ASTM C666 of a Pc of 60% by 300 cycles. Mixtures with CM were above this threshold until about 165 cycles, whereas those with SM were only able to be F/T resistant until roughly 130 cycles. All specimens were completely damaged by 270 cycles for CM mixtures and 235 cycles for SM mixtures. For C580 mixtures, both the plain mixture and the mixture with nS performed similarly to one another at approximately 300 cycles. On the contrary, similar to before, those mixtures with MS did not meet the Pc threshold of 60%. To be specific, they performed considerably

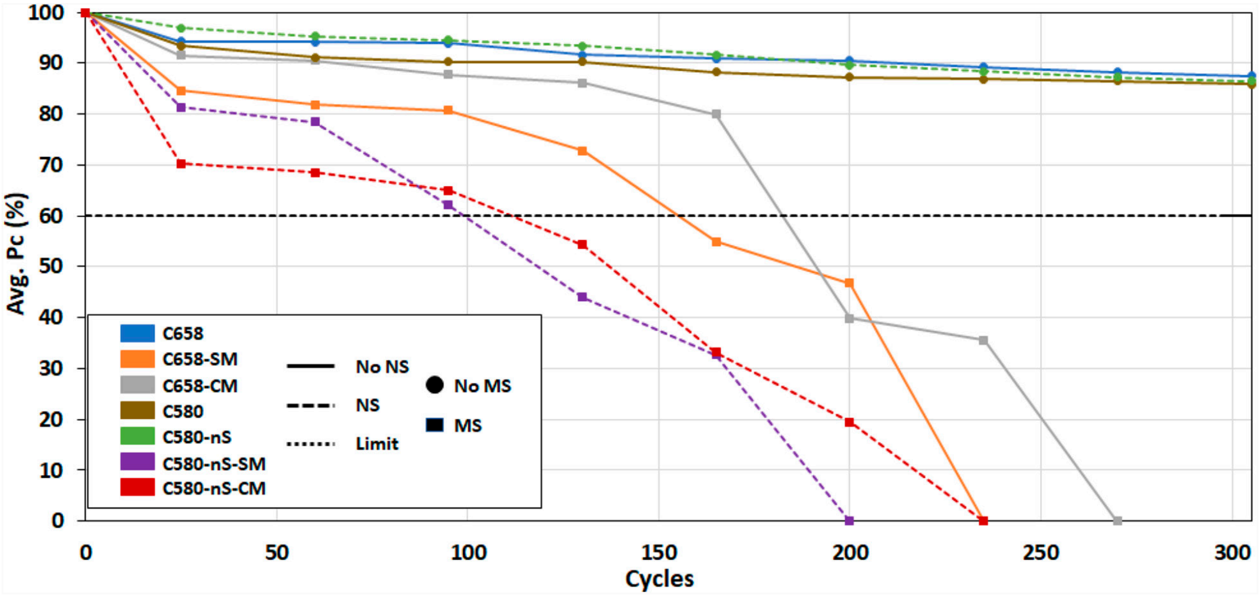

Figure 4.5 Freeze-Thaw Resistance of All Concrete Mixtures Compacted Using a Rod.

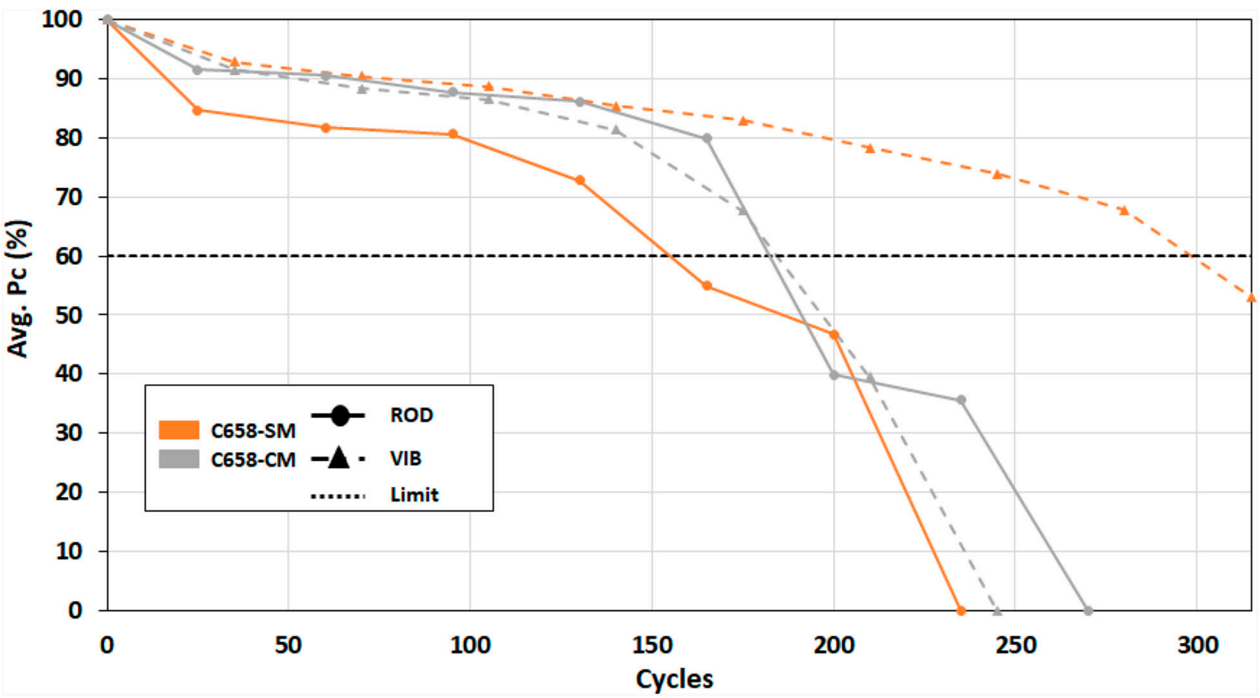

Figure 4.6 Freeze-Thaw Resistance of C658 Mixtures With MS Using Both Compaction Methods.

worse than before, given the lower cement content. At around 90 cycles, mixtures with MS barely met the threshold, and by ~200 cycles, they were too damaged to continue measurements. These results indicate that, at least in a lab setting, compacting the MS mixtures with a rod is not sufficient to guarantee F/T resistance.

The compaction method appeared to be highly beneficial for some C658 mixtures with MS (Figure 4.6). Precisely, when vibration was used, mixtures with SM achieved a PC of ~60% by 300 cycles. This was not observed when these mixtures were consolidated with a rod. It should be noted that despite meeting this threshold, the mixture with SM had a considerably lower Pc than the reference mixture. However, no apparent improvement was observed when vibration was used as the compaction effort for the mixtures with CM, as these performed similarly to when the mixtures were rodded.

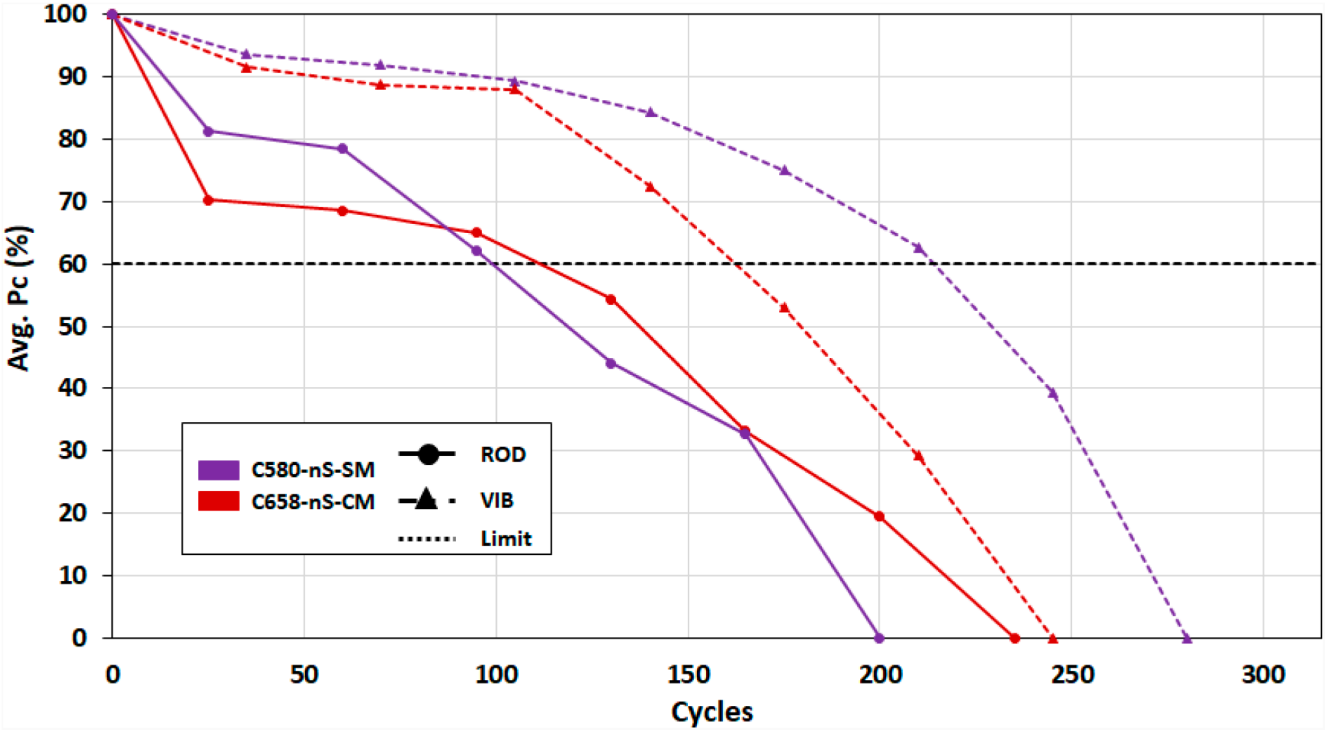

Figure 4.7 Freeze-Thaw Resistance of C580-nS Mixtures With MS Using Both Compaction Methods.

The efforts of compaction were considerably apparent for the C580 mixtures with nS and MS, as shown in Figure 4.7. Despite the evident increase in performance when vibration was used as the compaction method, mixtures with either SM or CM did not achieve a 60% Pc at 300 cycles. Specifically, mixtures with SM were slightly above this threshold at ~210 cycles, whereas mixtures with CM were below this threshold as soon as ~160 cycles. As observed in the C658 mixtures, those containing SM had a higher Pc than mixtures with CM. Lastly, these findings are consistent with the air-void system parameters observed for mixtures with MS. Consolidating them using vibration, rather than rodding, improved their air-void characteristics, but the mixtures still appear unlikely to provide fully adequate F/T resistance.

5. QUANTIFICATION OF THE CALCIUM HYDROXIDE REDUCTION FOR PASTE MIXTURES WITH AND WITHOUT COLLOIDAL NANOSILICA

5.1 Materials and Methods

5.1.1 Materials

Details regarding the materials used in this chapter have previously been discussed in Chapter 2. Microspheres were not used in this chapter. In addition to this, Class C fly ash meeting the specifications of ASTM C618-25 was used. The chemical composition of the Class C fly ash can be found in Table 5.1.

TABLE 5.1
Chemical Composition of Class C Fly Ash.

Composition	Wt. (%)
Al_2O_3	13.7
SiO_2	42.0
CaO	25.2
Fe_2O_3	9.3
MgO	2.0
SO_3	1.6

5.1.2 Testing Procedure

5.1.2.1 Thermogravimetric Analysis. The thermogravimetric analysis (TGA) was performed to determine the amount of CH in paste mixtures. For this purpose, paste specimens with and without nS were prepared with four different w/c ratios of 0.42, 0.44, 0.46, and 0.48 (R0.42, R0.44, R0.46, and R0.48, respectively). Paste specimens with Class C fly ash were cast at a 25% replacement level and a w/cm ratio of 0.44. These mixtures were cast in a plastic container and cured in a controlled chamber (23 °C (73 °F), 100% relative humidity) until their testing age (7, 28, and 56 days). At each testing age, the hardened paste samples were removed from the plastic containers, pieces were collected, and hydration was stopped. Approximately 16 mg of powder from the paste specimens was collected and analyzed. The CH content was determined by using the tangential line method (Kim & Olek, 2012).

5.2 Results and Discussions

5.2.1 Quantification of Calcium Hydroxide Reduction

The CH content of paste mixtures was determined at 7, 28, and 56 days and is shown in Figure 5.1. At 56 days, mixtures with higher w/c ratios generally achieved higher CH contents. In general, the use of nS reduced the CH content of mixtures relative to the corresponding baseline mixture at each w/c ratio. However, the amount of this reduction varied with w/c ratio and was relatively small in some cases. The mixture with w/c ratio of 0.46 (R0.46) appeared to show the highest CH reduction, whereas the mixture with w/c ratio of 0.44 (R0.44) had the least reduction. When comparing the mixtures with nS and those with Class C fly ash (CFA-25), it can be noted that the fly ash mixtures showed substantially lower CH content. This can be attributed to the combined dilution effect of 25% cement replacement and the inherently higher pozzolanic reactivity of Class C fly ash relative to nS.

The results from the CH consumption analysis (i.e., the reduction in CH with respect to its corresponding baseline mixture, and to the fly ash using R0.44 mixture as a reference) further corroborated the trends previously observed, as presented in Figure 5.2. Minimal CH consumption was observed at all ages for the R0.42-nS, R0.44-nS, and R0.46-nS mixtures, with 56-day consumptions of 2.7%, 0.3%, and 8.8%, respectively. However, the fly ash mixture (CFA-25) obtained a higher CH consumption than the nS mixtures at all ages.

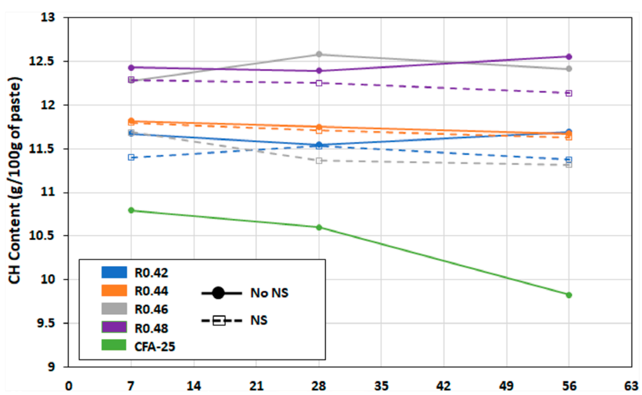

Figure 5.1 CH Content Amount in Paste Mixtures at 7, 28, and 56 Days.

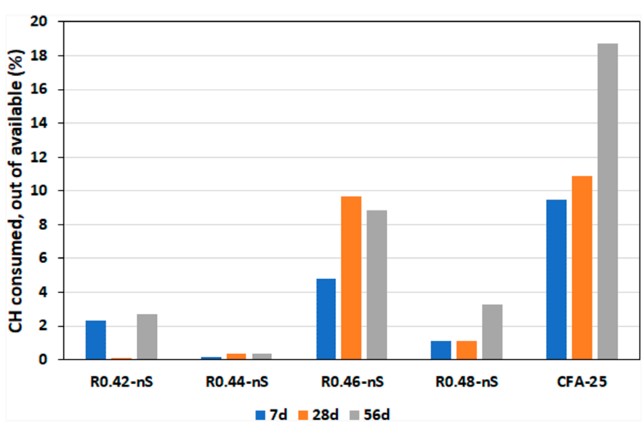

Figure 5.2 CH Consumed for Mixtures With nS Out of Available CH Based on the Respective Baseline Mixture.

6. EFFECT OF COLLOIDAL NANOSILICA ON AIR-VOID SYSTEM AND POROSITY OF CONCRETES AS A FUNCTION OF THE WATER-TO-CEMENT RATIO

6.1 Materials and Methods

6.1.1 Materials

Details regarding the materials used in this chapter have previously been discussed in Chapter 2. Microspheres were not used in this chapter.

6.1.2 Concrete Mixture Design

As previously stated, for bridge deck applications, INDOT utilizes Class C concrete (cement content of 658 lb/cyd (390 kg/m^3) and w/c ratio between 0.443 and 0.38). In this chapter, the objective was to develop bridge deck mixtures with reduced cement contents by adjusting the w/c ratio and evaluating the influence of colloidal nS on the air-void system and porosity. To do this, all mixtures were proportioned with a constant paste volume of 27%, while the cement and water contents were modified accordingly. In total, six concrete mixtures were selected: three mixtures with w/c ratios of 0.42, 0.46, and 0.48 and no nS, and three similar mixtures but with nS at the same w/c ratios. Table 6.1 summarizes all mixtures with and without nS. All mixtures were designed to achieve a slump of at least 3 in. (76 mm) with a tolerance of 0.5 in. (13 mm).

6.1.3 Testing Procedures

6.1.3.1 Slump and Fresh Air Content. Details regarding procedures used for the determination of slump and fresh air content are shown in Chapter 2.

6.1.3.2 Parameters of the Air-Void System in Hardened Concrete. Details regarding procedures used for the determination of the parameters of the air-void system in hardened concrete are presented in Chapter 2. An area of 12 in.^{2} (77 cm^2) was used for the analysis.

6.1.3.3 Compressive Strength. Details about the determination of the compressive strength of the specimens are provided in Chapter 2. At each testing age (7 and 28 days), three 4 × 8 in. (102 mm × 203 mm) cylinders were tested.

6.1.3.4 Rate of Water Absorption. Chapter 2 details the information regarding how the rate of water absorption experiment was conducted.

6.1.3.5 Density, Absorption, and Voids in Hardened Concrete. Disks measuring 4 × 2 (102 mm × 51 mm) in. were

TABLE 6.1
CMDs in SSD Conditions.

Mixture ID	Cement (lb/yd^3)	Water (lb/yd^3)	Fine Aggregate (lb/yd^3)	Coarse Aggregate (lb/yd^3)	WRA dosage (oz/cwt)	nS1 (oz/cwt)	nS2 (oz/cwt)
C610-0.42	610	257	1242	1704	7.9	N/A	N/A
C610-0.42-nS	610	257	1242	1704	10.3	4	8
C580-0.46	580	267	1242	1704	5.2	N/A	N/A
C580-0.46-nS	580	267	1242	1704	6.2	4	8
C566-0.48	566	272	1242	1704	4.7	N/A	N/A
C566-0.48-nS	566	272	1242	1704	5.7	4	8

NOTE: 1 lb/cyd = 0.593 kg/m^3, 1 oz/cwt = 65.2 mL/100kg.

cut from 4 × 8 in. (102 mm × 203 mm) cylinders and used to determine the density, total absorption, and total voids in hardened concrete per ASTM C642-21 (ASTM, 2021). The only modification to the procedure was that the specimens were vacuum-saturated in water at room temperature instead of being saturated using boiling water.

6.1.3.6 Freeze-Thaw Resistance. For information regarding how F/T resistance was conducted, please refer to Chapter 2. Three beams measuring 4 × 3 × 15.5 in. (102 × 76 × 394 mm) were tested for each mixture.

6.2 Results and Discussions

6.2.1 Slump

To reach the target slump of 3 ± 0.5 in. (76 ± 13 mm), all mixtures needed the use of WRA, as shown in Table 6.1. Mixtures with nS needed a considerably higher dosage of WRA to meet the target slump with respect to their baseline mixtures (see Figure 6.1). Specifically, all mixtures with nS needed approximately 20% or more in the amount of WRA used, with the highest increase of about 30% for the C610-0.42-nS mixture. This higher demand may likely be linked to the lower w/c ratio of this mixture compared with the others, as mixtures with higher and more similar w/c ratios showed comparable increases in WRA dosage. These findings suggest that special attention is needed when using colloidal nS, particularly at lower w/c ratios, to maintain adequate workability. The reason for the lower workability can be attributed to the high specific surface of nS.

6.2.2 Fresh and Hardened Air Content and Air-Void System Parameters

Mixtures with nS showed a larger reduction in hardened air content relative to their fresh air content than the corresponding reference mixtures (Figure 6.2), even though the fresh air contents were similar, and comparable AEA dosages were used. However, this greater loss in hardened air content is not necessarily detrimental. In the mixtures with nS, the air-void system became finer, as shown by the higher specific surface

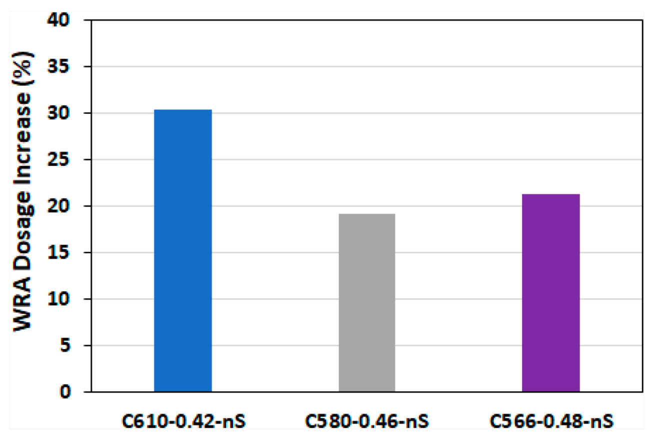

Figure 6.1 Increase in WRA Dosages for Mixtures With nS With Respect to Their Respective Baseline Mixture.

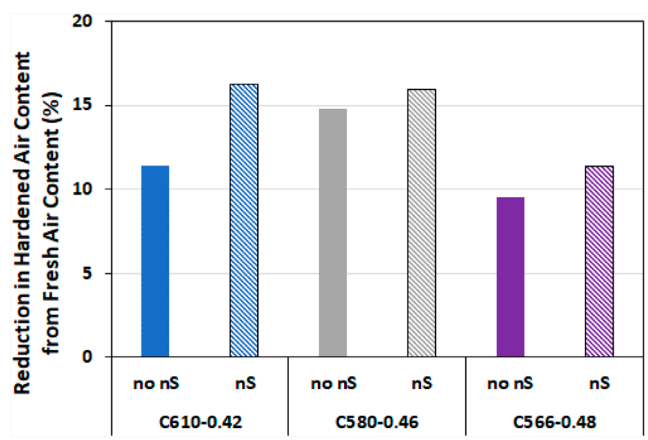

Figure 6.2 Reduction in Fresh Air Content From Hardened Air Content.

of the hardened voids (Figure 6.3). The combination of lower hardened air content and higher specific surface in the nS mixtures resulted in lower spacing factors compared with mixtures without nS (Table 6.2). Although the hardened air content was

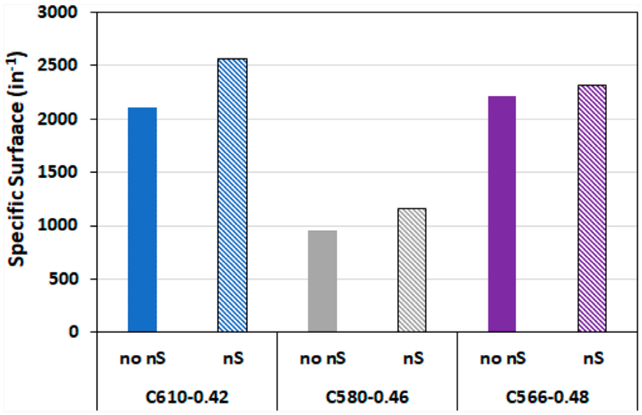

Figure 6.3 Specific Surface of Hardened Air Void in All Mixtures.
NOTE: 1 in.$^{-1}$ = 0.04 mm^{-1}

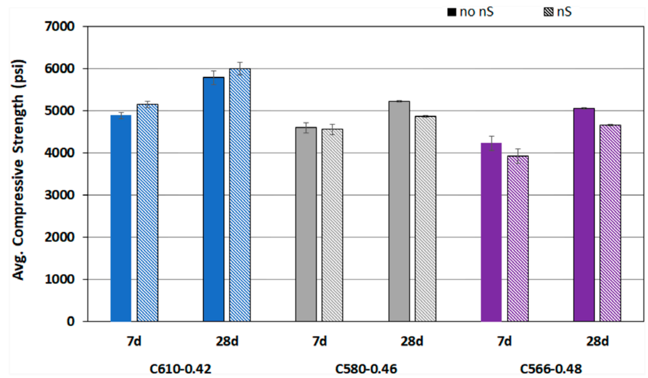

Figure 6.4 Compressive Strength of All Mixtures at 7 and 28 Days.
NOTE: 1 psi = 0.007 MPa.

TABLE 6.2
Air-Void System Parameters in Hardened Air Content.

Mixture ID	AEA (oz/cwt)	Fresh AC (%)	Hardened AC (%)	Reduction in Hardened AC (%)	Specific Surface (in.$^{-1}$)	Spacing Factor (in.)
C610-0.42	0.6	7.9	7.0	11.4	2106.4	0.0035
C610-0.42-nS	0.6	7.4	6.2	16.2	2561.9	0.0017
C580-0.46	0.5	6.1	5.2	14.8	954.5	0.0050
C580-0.46-nS	0.5	6.9	5.8	15.9	1162.2	0.0039
C566-0.48	0.4	6.3	5.7	9.5	2217.1	0.0061
C566-0.48-nS	0.4	7.9	7.0	11.4	2310.2	0.0047

NOTE: 1 oz/cwt = 65.2 mL/100kg, 1 in.$^{-1}$ = 0.04 mm^{-1}, 1 in. = 25.4 mm.

reduced, the resulting lower spacing factors are actually more desirable for protection against F/T damage.

6.2.3 *Compressive Strength*

The compressive strength at 7 and 28 days is presented in Figure 6.4. Among the reference concretes (without nS), the mixture with the highest cement content and lowest w/c ratio, C610-0.42, consistently had the highest strength at both ages. The C580-0.46 and C566-0.48 mixtures, which had lower cement contents and higher w/c ratios, showed very similar strengths to each other. A similar trend was observed for mixtures with nS. However, when evaluating the effects of nS, strength improvements were only noticeable for the C610-0.42 mixture, whereas the addition of nS to the C580-0.46 and C566-0.48 mixtures resulted in lower strengths. Overall, at the dosage evaluated, colloidal nS does not appear to substantially improve the compressive strength of these mixtures.

6.2.4 *Initial and Secondary Absorption*

The initial absorption results can be observed in Figure 6.5. Because initial absorption is largely influenced by the capillary porosity of the specimens (and porosity also influences compressive strength), the initial absorption results closely resembled the compressive strength trends. Mixtures with lower w/c ratios and higher cement contents exhibited lower initial absorption values, both with and without nS. However, the incorporation of nS did not improve the initial absorption. All mixtures with nS showed either similar or slightly higher initial absorption compared with their corresponding reference mixtures. Similar to the observed limited benefits for compressive strength, the colloidal nS dosage used in this study did not improve the initial water absorption performance of the mixtures.

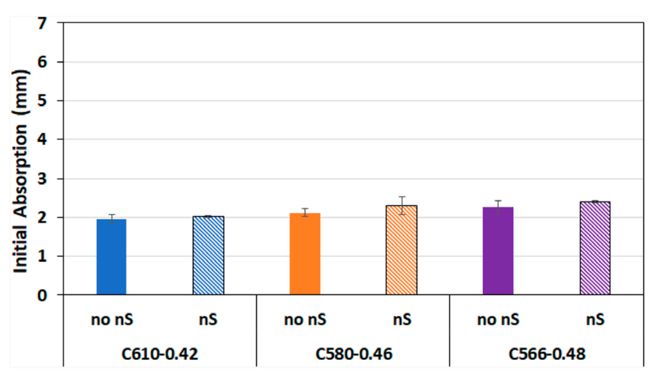

Figure 6.5 Initial Absorption for All Mixtures.
NOTE: 1 mm = 0.04 in.

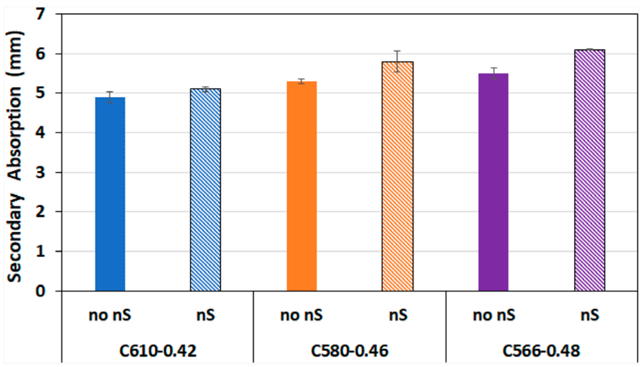

Figure 6.6 Secondary Absorption for All Mixtures.
NOTE: 1 mm = 0.04 in.

The secondary absorption results are shown in Figure 6.6. The C610-0.42 mixtures showed the lowest secondary absorption, while the C580-0.46 mixtures showed the highest values, with C566-0.48 falling in between. For all three w/c ratios, the inclusion of nS led to a slight increase in secondary absorption relative to the corresponding reference mixture, showcasing the minimal benefits of nS in terms of secondary absorption.

6.2.5 Density, Absorption, and Voids in Hardened Concrete

To further evaluate the impact of nS on capillary porosity, air-void content, and transport-related properties, measurements of density, absorption, and total void volume were assessed, as presented in Table 6.3. Among mixtures without nS, the permeable pore space increased progressively with the w/c ratio, from 15.64% in the C610-0.42 mixture to 18.78% in the C566-0.48 mixture. This trend is expected, as higher w/c ratios generally increase capillary porosity. This relationship is further supported by the hardened air content measurements, which were relatively close across the mixtures without nS: 7.0% for C610-0.42, 5.2% for C580-0.46, and 5.7% for C566-0.48. Although some variation exists, these values suggest that the increase in permeable pore space with a higher w/c ratio is primarily driven by capillary porosity rather than variations in entrained air content.

The effect of nS on permeable pore space varied depending on the type of mixture. In the lowest w/c ratio mixture (C610-0.42), the addition of nS slightly reduced the permeable pore space to 15.61%, a minimal change of 0.03% compared to the control. This small reduction may be attributed to the slightly lower hardened air content in the nS mixture (6.2% vs. 7.0%), which would decrease the total void volume and thus the measured permeable pore space. This result is consistent with the improvement of compressive strength in the C610-0.42 mixture with nS.

In contrast, the C580-0.46-nS mixture showed a moderate increase in permeable pore space (from 17.86% to 18.54%). This coincided with a higher hardened air content and greater total absorption after saturating the samples with water, suggesting a more connected pore network.

For the highest w/c ratio mixture (C566-0.48), the addition of nS decreased the permeable pore space (from 18.78% to 17.67%), despite considerably higher hardened air content. This indicates that while nS may contribute to densification, its influence in mixtures with a higher w/c ratio appears to be more strongly related to modification in the variation of void size and distribution. These changes likely affected the overall connectivity of the pore network, leading to different effects on permeable pore space in the C580 and C566 mixtures.

The absorption after immersion and vacuum saturation, and the apparent density values showcase that nS influences the void structure more than the matrix itself for these mixtures. For the C610-0.42 mixture, nS showed a slightly lower absorption and slightly higher density, suggesting a modest densification effect. In contrast, the C580-0.46 mixture showed increased absorption and reduced density with nS. The C566-0.48 mixture displayed reduced vacuum absorption and reduced density with nS, yet still exhibited higher secondary absorption. These results showcase that changes in the void network played a role in transport behavior, especially in mixtures with nS and higher w/c.

6.2.6 Freeze-Thaw Resistance

The inclusion of nS in the mixtures appeared to improve the F/T performance relative to the baseline mixtures without nS, as shown in Figure 6.7. As expected, mixtures with lower w/c ratios generally showed better performance because of their lower porosity, regardless of whether nS was used. The benefit of nS was more noticeable in the mixture with the highest w/c ratio, C566-0.48, where Pc increased by about 10% at 300 cycles in the C566-0.48-nS mixture compared with its control.

TABLE 6.3
Summary of Absorption and Air-Void Space Characteristics.

Mixture ID	Hardened AC (%)	Volume of Permeable Pore Space (%)	Absorption after Immersion and Vacuuming (%)	Apparent Density (g/cm^3)
C610-0.42	7.0	15.64	7.25	2.56
C610-0.42-nS	6.2	15.61	7.17	2.58
C580-0.46	5.2	17.86	8.47	2.57
C580-0.46-nS	5.8	18.54	9.04	2.51
C566-0.48	5.7	18.78	8.91	2.60
C566-0.48-nS	7.0	17.67	8.48	2.54

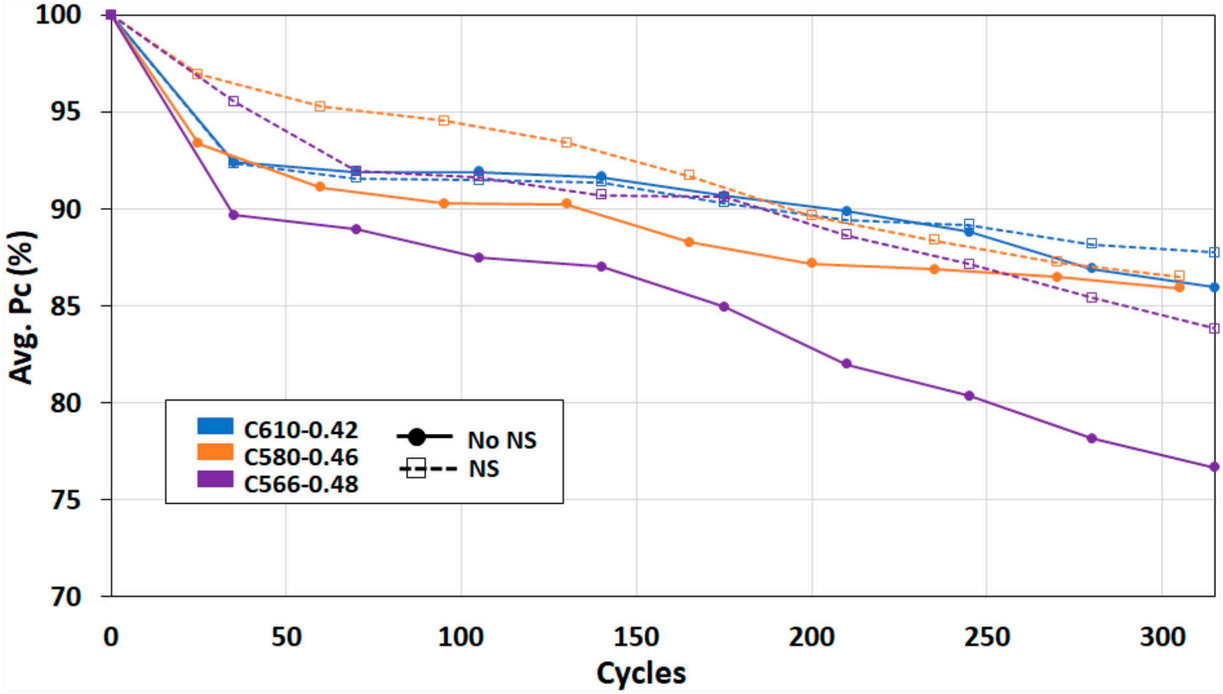

Figure 6.7 Freeze-Thaw Resistance for All Mixtures.

For the C610-0.42 and C580-0.46 mixtures, the use of nS also resulted in Pc increases of approximately 2%. Overall, these improvements in F/T resistance, albeit slight in some instances, can be attributed to the refinement of the hardened air-void system, as nS refined the void system and reduced spacing factors, offsetting the overall reduction in hardened air content relative to the mixtures without nS.

7. CONCLUSIONS

7.1 Findings

7.1.1 Field Trials of Concrete Mixtures With Colloidal Nanosilica and Alternative (Microspheres) Air-Entrainment Products

- Despite truck tickers showing lower than target values w/c ratio (0.35–0.41 vs. 0.44 and 0.36–0.44 vs 0.46), all mixtures achieved adequate slumps.
- SM mixtures produced more desirable air-void system characteristics (higher void frequency, shorter chord length, greater specific surface, and lower spacing factor) than CM mixtures. The method of mixing (wet vs. dry) also influenced the F/T performance of these mixtures.
- Mixtures with MS achieved compressive and flexural strengths comparable to or higher than the reference mixtures, with CM mixtures often producing the highest strengths. In contrast, those with MS and nS had lower performance in comparison to the plain reference mixture.
- Mixtures with MS reduced secondary water absorption, and when used in conjunction with nS improved the chloride penetration performance.
- In F/T testing, all C658 mixtures except C658-CM-W met the threshold of 60% for durability factor (DF) at 300 cycles, with SM performing best. Nanosilica improved F/T resistance of reference mixtures, while mixtures with both nS and MS met the minimum threshold.

7.1.2 Production of Laboratory Specimens Using Variable Consolidation Methods to Assess the Effects of Colloidal Nanosilica and Microspheres on the Fresh, Mechanical, and Durability Properties of Concrete

- Vibration improved MS dispersion, as indicated by the frequency and specific surface parameters relative to when the mixtures were rodded. However, mixtures with MS did not achieve the dispersion required for reliable entrained-air protection as defined by the dispersion factor criteria reported in the literature (the dispersion factor must be equal to or greater than 10 times the paste content by volume).
- Mixtures with MS required substantially higher WRA dosage, with CM needing the highest amount. The addition of nS further increased WRA demand.
- Mixtures with MS increased the compressive strength at all ages. Similarly, mixtures incorporating both MS and nS achieved higher compressive strength compared to mixtures containing only nS. In contrast, mixtures with only nS did not improve the compressive strength and were often lower in comparison to their control mixture.
- In F/T testing, none of the rodded MS mixtures reached a DF greater than 60% at 300 cycles. When vibration was used for consolidation, the C658-SM mixture reached a DF of approximately 60% at 300 cycles while all others failed to meet this threshold. In contrast, mixtures with nS showed an adequate F/T resistance (DF > 85% at 300 cycles).

7.1.3 Quantification of the Calcium Hydroxide Reduction for Paste Mixtures With and Without Colloidal Nanosilica

- Nanosilica reduced the CH content of paste mixtures at all ages and w/c ratios, but the magnitude of the reduction was generally very low. CH consumption values at 56 days were low (0.3% to 8.8%), indicating limited pozzolanic reaction of nS at the studied dosage. The highest reduction in CH was observed for the mixture with a w/c ratio of 0.46
- Class C fly ash reduced CH content of paste mixtures far more effectively than nS due to its higher pozzolanic reactivity and dilution effect. These mixtures showed a considerably higher CH consumption at all ages than nS mixtures.

7.1.4 Effect of Colloidal Nanosilica on Air-Void System and Porosity of Concretes as a Function of the Water-to-Cement Ratio

- Mixtures with nS increased WRA demand by 20% to 30% compared to the reference mixtures, with the highest demand observed at the lowest w/c ratio. These mixtures also experienced greater reductions in air content from fresh to hardened state, but developed finer void systems with higher specific surface values.
- Mixtures with nS consistently reduced spacing factors relative to corresponding baselines, thus theoretically improving F/T protection despite a generally lower hardened air content.
- Mixtures with nS slightly improved compressive strength only at a w/c ratio of 0.42, while slightly decreased strength at w/c ratios of 0.46 and 0.48.
- Nanosilica did not reduce initial or secondary absorption of concrete mixtures and, depending on the w/c ratio, sometimes increased permeable pore space as indicated by ASTM C642-21.
- In terms of F/T resistance, mixtures with nS showed improvements across all w/c ratios, with the highest increase observed in the mixture with a w/c ratio of 0.48. These results were in agreement with those seen for the parameters of the air-void system.

7.2 Recommendations and Future Work

Results of this study showed that both MS and nS can influence the durability performance of concrete in different ways. Mixtures with MS were able to increase compressive strength and reduce secondary rates of water absorption, and in certain cases (particularly SM mixtures), they may be able to perform adequately against F/T damage at the cement content studied (658 lb/cyd [390 kg/m^3]). Mixtures with nS refined the air-void system and provided modest improvements in F/T resistance, especially at higher w/c ratios. However, the findings also demonstrated that these benefits are highly sensitive to mixture proportioning, consolidation method, and dispersion.

The results also indicated that the MS mixtures prepared in the lab with nS do not achieve an adequate dispersion. For mixtures with nS, at least in the lab, benefits were not noticeable in terms of strength or selected durability parameters, indicating that the current dosage may not be sufficient. Mixtures with lower cement contents (580 lb/cyd [344 kg/m^3]) showed particular performance challenges when MS and nS were used in combination.

Based on the findings of this research, successful implementation of MS and nS admixtures in full-scale concrete construction would benefit from addressing the following issues:

- Field trials should be repeated with correct w/c ratios to fully understand the benefits and limitations of nS and MS in a practical setting.
- The mechanisms controlling the dispersion and stability of MS (especially for CM) should be further investigated, as inadequate dispersion was closely linked to poor F/T resistance despite otherwise increased compressive strength performance.
- Before broad implementation, further research is needed to optimize nS dosage for different w/c ratios, as nS improved F/T resistance mainly at higher w/c but did not enhance mechanical or transport properties at lower w/c ratios.
- Interactions between nS, MS, and chemical admixtures (especially WRAs and AEAs) should be studied, given the significant increase in WRA demand and the observed reduction in hardened air content in nS mixtures.
- Long-term durability testing, such as scaling resistance, carbonation, creep, and shrinkage, may be necessary to validate laboratory trends and ensure that MS and nS enhance performance under field conditions.

REFERENCES

ASTM International. (2015). *Standard test method for resistance of concrete to rapid freezing and thawing* (ASTM C666/C666M-15). https://doi.org/10.1520/C0666_C0666M-15

ASTM International. (2020a). *Standard test method for acid-soluble chloride in mortar and concrete* (ASTM C1152/C1152M-20). https://doi.org/10.1520/C1152_C1152M-20

ASTM International. (2020b). *Standard test method for measurement of rate of absorption of water by hydraulic-cement concretes* (ASTM C1585-20). https://doi.org/10.1520/C1585-20

ASTM International. (2020c). *Standard test method for obtaining and testing drilled cores and sawed beams of concrete* (ASTM C42/C42M-20). https://doi.org/10.1520/C0042_C0042M-20

ASTM International. (2020d). *Standard test method for slump of hydraulic-cement concrete* (ASTM C143/C143M-20). https://doi.org/10.1520/C0143_C0143M-20

ASTM International. (2021). *Standard test method for density, absorption, and voids in hardened concrete* (ASTM C642-21). https://doi.org/10.1520/C0642-21

ASTM International. (2022a). *Standard test method for Dynamic Youngs Modulus, Shear Modulus, and Poisson's Ratio by impulse excitation of vibration* (ASTM E1876-22). https://doi.org/10.1520/E1876-22

ASTM International. (2022b). *Standard test method for flexural strength of concrete (using simple beam with third-point loading)* (ASTM C78/C78M-22). https://doi.org/10.1520/C0078_C0078M-22

ASTM International. (2023). *Standard test method for air content of freshly mixed concrete by the volumetric method* (ASTM C173/C173M-23). https://doi.org/10.1520/C0173_C0173M-23

ASTM International. (2024a). *Standard test method for air content of freshly mixed concrete by the pressure method* (ASTM C231/C231M-24). https://doi.org/10.1520/C0231_C0231M-24

ASTM International. (2024b). *Standard specification for air-entraining admixtures for concrete* (ASTM C260/C260M-24). https://doi.org/10.1520/C0260_C0260M-24

ASTM International. (2024c). *Standard specification for blended hydraulic cements* (ASTM C595/C595M-24). https://doi.org/10.1520/C0595_C0595M-24

ASTM International. (2024d). *Standard specification for chemical admixtures for concrete* (ASTM C494/C494M-24). https://doi.org/10.1520/C0494_C0494M-24

ASTM International. (2024e). *Standard test method for compressive strength of cylindrical concrete specimens* (ASTM C39/C39M-24). https://doi.org/10.1520/C0039_C0039M-24

ASTM International. (2024f). *Standard test method for microscopical determination of parameters of the air-void system in hardened concrete* (ASTM C457/C457M-24). https://doi.org/10.1520/C0457_C0457M-24

Attiogbe, E. K. (2021). A new way to deliver protection from freezing-and-thawing damage *Concrete International*, *43*(1), 27–33. https://doi.org/10.14359/51730453

Attiogbe, E. K. (2022). Microspheres in hardened concrete. *Concrete International*, *44*(3), 43–50. https://doi.org/10.14359/51734624

Björnström, J., Martinelli, A., Matic, A., Börjesson, L., & Panas, I. (2004). Accelerating effects of colloidal nano-silica for beneficial calcium–silicate–hydrate formation in cement. *Chemical Physics Letters*, *392*(1–3), 242–248. https://doi.org/10.1016/j.cplett.2004.05.071

Chen, J., Kou, S.-c., & Poon, C.-s. (2012). Hydration and properties of nano-TiO_2 blended cement composites. *Cement and Concrete Composites*, *34*(5), 642–649. https://doi.org/10.1016/J.CEMCONCOMP.2012.02.009

Chuah, S., Pan, Z., Sanjayan, J. G., Wang, C. M., & Duan, W. H. (2014). Nano reinforced cement and concrete composites and new perspective from graphene oxide. *Construction and Building Materials*, *73*, 113–124. https://doi.org/10.1016/J.CONBUILDMAT.2014.09.040

Fernández, J. M., Duran, A., Navarro-Blasco, I., Lanas, J., Sirera, R., & Alvarez, J. I. (2013). Influence of nanosilica and a polycarboxylate ether superplasticizer on the performance of lime mortars. *Cement and Concrete Research*, *43*, 12–24. https://doi.org/10.1016/j.cemconres.2012.10.007

Huang, D., Velay-Lizancos, M., & Olek, J. (2022). *Improving scaling resistance of pavement concrete using titanium dioxide (TiO_2) and nanosilica* (Joint Transportation Research Program Publication No. FHWA/IN/JTRP-2022/32). Purdue University. https://doi.org/10.5703/1288284317583

Indiana Department of Transportation. (2022). *Standard specifications: Division 700 – Structures*. https://www.in.gov/dot/div/contracts/standards/book/sep21/700-2022.pdf

Indiana Department of Transportation. (2024). *Standard specifications: Division 900 – Materials*. https://www.in.gov/dot/div/contracts/standards/book/sep23/900-2024.pdf

Kim, T., & Olek, J. (2012). Effects of sample preparation and interpretation of thermogravimetric curves on calcium hydroxide in hydrated pastes and mortars. *Transportation Research Record*, *2290*(1), 10–18. https://doi.org/10.3141/2290-02

Kong, D., Su, Y., Du, X., Yang, Y., Wei, S., & Shah, S. P. (2013). Influence of nano-silica agglomeration on fresh properties of cement pastes. *Construction and Building Materials*, *43*, 557–562. https://doi.org/10.1016/j.conbuildmat.2013.02.066

Konsta-Gdoutos, M. S., Metaxa, Z. S., & Shah, S. P. (2010). Highly dispersed carbon nanotube reinforced cement based materials. *Cement and Concrete Research*, *40*(7), 1052–1059. https://doi.org/10.1016/j.cemconres.2010.02.015

Lee, B. Y., & Kurtis, K. E. (2010). Influence of TiO_2 nanoparticles on early C_3S hydration. *Journal of the American Ceramic Society*, *93*(10), 3399–3405. https://doi.org/10.1111/J.1551-2916.2010.03868.X

Liew, K. M., Kai, M. F., & Zhang, L. W. (2016). Carbon nanotube reinforced cementitious composites: An overview. *Composites Part A: Applied Science and Manufacturing*, *91*, 301–323. https://doi.org/10.1016/j.compositesa.2016.10.020

Maglad, A. M., Zaid, O., Arbili, M. M., Ascensão, G., Şerbănoiu, A. A., Grădinaru, C. M., García, R. M., Qaidi, S. M. A., Althoey, F., & de Prado-Gil, J. (2022). A study on the properties of geopolymer concrete modified with nano graphene oxide. *Buildings*, *12*(8), 1066. https://doi.org/10.3390/buildings12081066

Meng, W., & Khayat, K. H. (2018). Effect of graphite nanoplatelets and carbon nanofibers on rheology, hydration, shrinkage, mechanical properties, and microstructure of UHPC. *Cement and Concrete Research*, *105*, 64–71. https://doi.org/10.1016/j.cemconres.2018.01.001

Metaxa, Z. S., Konsta-Gdoutos, M. S., & Shah, S. P. (2013). Carbon nanofiber cementitious composites: Effect of debulking procedure on dispersion and reinforcing efficiency. *Cement and Concrete Composites*, *36*(1), 25–32. https://doi.org/10.1016/J.CEMCONCOMP.2012.10.009

Moro, C., Francioso, V., & Velay-Lizancos, M. (2021). Impact of nano-TiO_2 addition on the reduction of net CO_2 emissions of cement pastes after CO_2 curing. *Cement and Concrete Composites*, *123*. https://doi.org/10.1016/J.CEMCONCOMP.2021.104160

Musso, S., Tulliani, J.-M., Ferro, G., & Tagliaferro, A. (2009). Influence of carbon nanotubes structure on the mechanical behavior of cement composites. *Composites Science and Technology*, *69*(11–12), 1985–1990. https://doi.org/10.1016/j.compscitech.2009.05.002

Nili, M., & Ehsani, A. (2015). Investigating the effect of the cement paste and transition zone on strength development of concrete containing nanosilica and silica fume. *Materials & Design*, *75*, 174–183. https://doi.org/10.1016/j.matdes.2015.03.024

Noorvand, H., Abang Ali, A. A., Demirboga, R., Farzadnia, N., & Noorvand, H. (2013). Incorporation of nano TiO_2 in black rice husk ash mortars. *Construction and Building Materials*, *47*, 1350–1361. https://doi.org/10.1016/J.CONBUILDMAT.2013.06.066

P. P., A., Nayak, D. K., Sangoju, B., Kumar, R., & Kumar, V. (2021). Effect of nano-silica in concrete; a review. *Construction and Building Materials*, *278*. https://doi.org/10.1016/j.conbuildmat.2021.122347

Peyvandi, A., Sbia, L. A., Soroushian, P., & Sobolev, K. (2013). Effect of the cementitious paste density on the performance efficiency of carbon nanofiber in concrete nanocomposite. *Construction and Building Materials*, *48*, 265–269. https://doi.org/10.1016/j.conbuildmat.2013.06.094

Said, A. M., Zeidan, M. S., Bassuoni, M. T., & Tian, Y. (2012). Properties of concrete incorporating nano-silica. *Construction and Building Materials*, *36*, 838–844. https://doi.org/10.1016/J.CONBUILDMAT.2012.06.044

Shah, S. P., Hou, P., & Konsta-Gdoutos, M. S. (2015). Nano-modification of cementitious material: Toward a stronger and durable concrete. *Journal of Sustainable Cement-Based Materials*, *5*(1), 1–22. https://doi.org/10.1080/21650373.2015.1086286

Singh, L. P., Karade, S. R., Bhattacharyya, S. K., Yousuf, M. M., & Ahalawat, S. (2013). Beneficial role of nanosilica in cement based materials – A review. *Construction and Building Materials*, *47*, 1069–1077. https://doi.org/10.1016/j.conbuildmat.2013.05.052

Tong, T., Fan, Z., Liu, Q., Wang, S., Tan, S., & Yu, Q. (2016). Investigation of the effects of graphene and graphene oxide nanoplatelets on the micro- and macro-properties of cementitious materials. *Construction and Building Materials*, *106*, 102–114. https://doi.org/10.1016/j.conbuildmat.2015.12.092

Yang, Z., He, R., Tan, Y., Chen, H., & Cao, D. (2021). Air pore structure, strength and frost resistance of air-entrained mortar with different dosage of nano-SiO_2 hydrosol. *Construction and Building Materials*, *308*. https://doi.org/10.1016/j.conbuildmat.2021.125096

About the Joint Transportation Research Program (JTRP)

On March 11, 1937, the Indiana Legislature passed an act which authorized the Indiana State Highway Commission to cooperate with and assist Purdue University in developing the best methods of improving and maintaining the highways of the state and the respective counties thereof. That collaborative effort was called the Joint Highway Research Project (JHRP). In 1997 the collaborative venture was renamed as the Joint Transportation Research Program (JTRP) to reflect the state and national efforts to integrate the management and operation of various transportation modes.

The first studies of JHRP were concerned with Test Road No. 1—evaluation of the weathering characteristics of stabilized materials. After World War II, the JHRP program grew substantially and was regularly producing technical reports. Over 1,600 technical reports are now available, published as part of the JHRP and subsequently JTRP collaborative venture between Purdue University and what is now the Indiana Department of Transportation.

Free online access to all reports is provided through a unique collaboration between JTRP and Purdue Libraries. These are available at docs.lib.purdue.edu/jtrp/.

Further information about JTRP and its current research program is available at engineering.purdue.edu/JTRP.

About This Report

An open access version of this publication is available online. See the URL in the citation below.

Castillo, A., Olek, J., & Velay-Lizancos, M. (2026). *Influence of nanomaterials-based admixtures and polymeric microspheres on entrained air void system and freeze-thaw (F/T) resistance of concrete* (Joint Transportation Research Program Publication No. FHWA/IN/JTRP-2026/13). West Lafayette, IN: Purdue University. https://doi.org/10.5703/1288284318621